# SPT-3G: A Next-Generation Cosmic Microwave Background Polarization Experiment on the South Pole Telescope

B. A. Benson[a,b,c], P. A. R. Ade[d], Z. Ahmed[e,f,g], S. W. Allen[e,f,g], K. Arnold[h], J. E. Austermann[i]
, A. N. Bender[j], L. E. Bleem[b,k], J. E. Carlstrom[b,l,m,k,c], C. L. Chang[k,b,c], H. M. Cho[g],
S. T. Ciocys[k], J. F. Cliche[j], T. M. Crawford[b,c], A. Cukierman[n], T. de Haan[j], M. A. Dobbs[j,o],
D. Dutcher[b,m], W. Everett[i], A. Gilbert[j], N. W. Halverson[i,p], D. Hanson[j], N. L. Harrington[n],
K. Hattori[q], J. W. Henning[i], G. C. Hilton[r], G. P. Holder[j,o], W. L. Holzapfel[n], K. D. Irwin[e,f,g],
R. Keisler[e,f], L. Knox[s], D. Kubik[a], C. L. Kuo[e,f,g], A. T. Lee[n,t], E. M. Leitch[b,c], D. Li[r],
M. McDonald[u], S. S. Meyer[b,l,m,c], J. Montgomery[j], M. Myers[n], T. Natoli[b,m], H. Nguyen[a],
V. Novosad[v], S. Padin[w], Z. Pan[b,m], J. Pearson[v], C. L. Reichardt[x,n], J. E. Ruhl[y],
B. R. Saliwanchik[y], G. Simard[j], G. Smecher[z], J. T. Sayre[y], E. Shirokoff[b,c], A. A. Stark[aa],
K. Story[b,m], A. Suzuki[n], K. L. Thompson[e,f,g], C. Tucker[d], K. Vanderlinde[bb,cc], J. D. Vieira[dd,ee]
, A. Vikhlinin[aa], G. Wang[k], V. Yefremenko[k], K. W. Yoon[e,f,g]

[a]Fermi National Accelerator Laboratory, MS209, P.O. Box 500, Batavia, IL 60510-0500
[b]Kavli Institute for Cosmological Physics, University of Chicago, 5640 South Ellis Avenue, Chicago, IL 60637
[c]Department of Astronomy and Astrophysics, University of Chicago, 5640 South Ellis Avenue, Chicago, IL 60637
[d]School of Physics and Astronomy, Cardiff University, Cardiff CF24 3YB, United Kingdom
[e]Kavli Institute for Particle Astrophysics and Cosmology, Stanford University, 452 Lomita Mall, Stanford, CA 94305
[f]Department of Physics, Stanford University, 382 Via Pueblo Mall, Stanford, CA 94305
[g]SLAC National Accelerator Laboratory, 2575 Sand Hill Road, Menlo Park, CA 94025
[h]Department of Physics, University of California, San Diego, CA 92093
[i]CASA, Department of Astrophysical and Planetary Sciences, University of Colorado, Boulder, Colorado 80309, USA
[j]Department of Physics, McGill University, 3600 Rue University, Montreal, Quebec H3A 2T8, Canada
[k]Argonne National Laboratory, High-Energy Physics Division, 9700 S. Cass Avenue, Argonne, IL, USA 60439
[l]Enrico Fermi Institute, University of Chicago, 5640 South Ellis Avenue, Chicago, IL 60637
[m]Department of Physics, University of Chicago, 5640 South Ellis Avenue, Chicago, IL 60637
[n]Department of Physics, University of California, Berkeley, CA 94720
[o]Canadian Institute for Advanced Research, CIFAR Program in Cosmology and Gravity, Toronto, ON, M5G 1Z8, Canada
[p]Department of Physics, University of Colorado, Boulder, CO 80309
[q]High Energy Accelerator Research Organization (KEK), Tsukuba, Ibaraki 305-0801, Japan
[r]NIST Quantum Devices Group, 325 Broadway Mailcode 817.03, Boulder, CO, USA 80305
[s]Department of Physics, University of California, One Shields Avenue, Davis, CA 95616
[t]Physics Division, Lawrence Berkeley National Laboratory, Berkeley, CA 94720
[u]Kavli Institute for Astrophysics and Space Research, Massachusetts Institute of Technology, 77 Massachusetts Avenue, Cambridge, MA 02139
[v]Argonne National Laboratory, Material Science Division, 9700 S. Cass Avenue, Argonne, IL, USA 60439
[w]California Institute of Technology, 1200 E. California Blvd., Pasadena, CA 91125
[x]School of Physics, University of Melbourne, Parkville, 3010 VIC, Australia
[y]Physics Department, Case Western Reserve University, Cleveland, OH 44106
[z]Three-Speed Logic, Inc., Vancouver, B.C., V6A 2J8, Canada
[aa]Harvard-Smithsonian Center for Astrophysics, 60 Garden Street, Cambridge, MA 02138
[bb]Dunlap Institute for Astronomy & Astrophysics, University of Toronto, 50 St George St, Toronto, ON, M5S 3H4, Canada
[cc]Department of Astronomy & Astrophysics, University of Toronto, 50 St George St, Toronto, ON, M5S 3H4, Canada
[dd]Astronomy Department, University of Illinois, 1002 W. Green Street, Urbana, IL 61801 USA
[ee]Department of Physics,University of Illinois, 1110 W. Green Street, Urbana, IL 61801 USA

## ABSTRACT

We describe the design of a new polarization sensitive receiver, SPT-3G, for the 10-meter South Pole Telescope (SPT). The SPT-3G receiver will deliver a factor of ∼20 improvement in mapping speed over the current receiver,

Further author information: (Send correspondence to B.A. Benson)
E-mail: bbenson@kicp.uchicago.edu, Telephone: 1 773 702 6452

SPT-POL. The sensitivity of the SPT-3G receiver will enable the advance from statistical detection of $B$-mode polarization anisotropy power to high signal-to-noise measurements of the individual modes, i.e., maps. This will lead to precise ($\sim0.06\,\mathrm{eV}$) constraints on the sum of neutrino masses with the potential to directly address the neutrino mass hierarchy. It will allow a separation of the lensing and inflationary $B$-mode power spectra, improving constraints on the amplitude and shape of the primordial signal, either through SPT-3G data alone or in combination with BICEP2/KECK, which is observing the same area of sky. The measurement of small-scale temperature anisotropy will provide new constraints on the epoch of reionization. Additional science from the SPT-3G survey will be significantly enhanced by the synergy with the ongoing optical Dark Energy Survey (DES), including: a 1% constraint on the bias of optical tracers of large-scale structure, a measurement of the differential Doppler signal from pairs of galaxy clusters that will test General Relativity on $\sim200\,\mathrm{Mpc}$ scales, and improved cosmological constraints from the abundance of clusters of galaxies.

**Keywords:** B-modes, cosmic microwave background, cryogenics, inflation, gravitational lensing, neutrino mass, optical design, polarization, transition-edge sensors

# 1. INTRODUCTION

The SPT is a 10 meter telescope optimized for sensitive, high-resolution measurements of the CMB anisotropy and mm-wave sky.[1,2] The telescope is located at the NSF Amundsen-Scott South Pole station, one of the best developed sites on Earth for mm-wave observations, with particularly low levels of atmospheric fluctuation power on degree angular scales.[3,4] The telescope is an off-axis, classical Gregorian design which gives a wide diffraction-limited field of view, low scattering, and high efficiency with no blockage of the primary aperture. The current telescope optics produce a $1'$ FWHM beamwidth at 150 GHz with a conservative illumination of the inner 8 meters of the telescope, and a $\sim1$ deg$^2$ diffraction-limited field of view.[5] The SPT is designed to modulate the beams on the sky by slewing the entire telescope at up to 4 deg s$^{-1}$, eliminating the need for a chopping mirror. The telescope operates largely remotely, with a high observing efficiency.

The SPT has thus far been used for two surveys: 1) the completed 2500 deg$^2$ SPT-SZ survey[6] (2007-2011), and 2) the ongoing 500 deg$^2$ SPT-POL survey[7] (2012-2015). The SPT-SZ survey observed 2500 deg$^2$ of sky with an unprecedented combination of angular resolution ($\sim1$ arcmin) and depth at mm-wavelengths, achieving a noise level of approximately 36, 16, and 62 $\mu$K-arcmin[*] at 95, 150, and 220 GHz, respectively .[8] The SPT-POL survey observes at 95 and 150 GHz, with added polarization sensitivity. By the end of 2015, the SPT-POL survey is expected to have observed 500 deg$^2$ of sky to a depth of 6 $\mu$K-arcmin at 150 GHz, a noise level approximately seven times lower than the 143 GHz *Planck* first data release. In Figure 1, we show a 30 deg$^2$ cut-out of a SPT-POL map observed to full survey depth, which illustrates the improvements in resolution and depth of the SPT-POL data in comparison to WMAP and *Planck*. The SPT-SZ and SPT-POL observations have led to significant results and new discoveries in three main areas: using the SZ effect to discover new galaxy clusters (particularly at high redshift) ,[9–13] the systematic discovery of strongly lensed high-redshift star forming galaxies ,[14–16] measurements of the fine-scale CMB temperature anisotropy ,[6,17–21] and the first detection of the so-called "$B$ modes" in the polarization of the CMB.[22]

The third-generation camera for the SPT, SPT-3G, will exploit the full power of ground-based CMB observations. The SPT-3G camera will exploit two technological advances to achieve the necessary leap in sensitivity: 1) an improved wide-field optical design that allows more than twice as many diffraction-limited optical elements in the focal plane, and 2) multi-chroic pixels that are sensitive to multiple observing bands in a single detector element. The combination of these two advances will deliver a factor-of-20 improvement in mapping speed over the already impressive SPT-POL camera. The SPT-3G survey will observe for four years, from 2016-2019, and cover 2500 deg$^2$: an area equal to the original SPT-SZ survey but observed at a noise level 10$\times$ lower in temperature. In Section 2, we discuss the scientific motivation for SPT-3G. In Section 3, we discuss the instrumentation development necessary to achieve these goals.

---

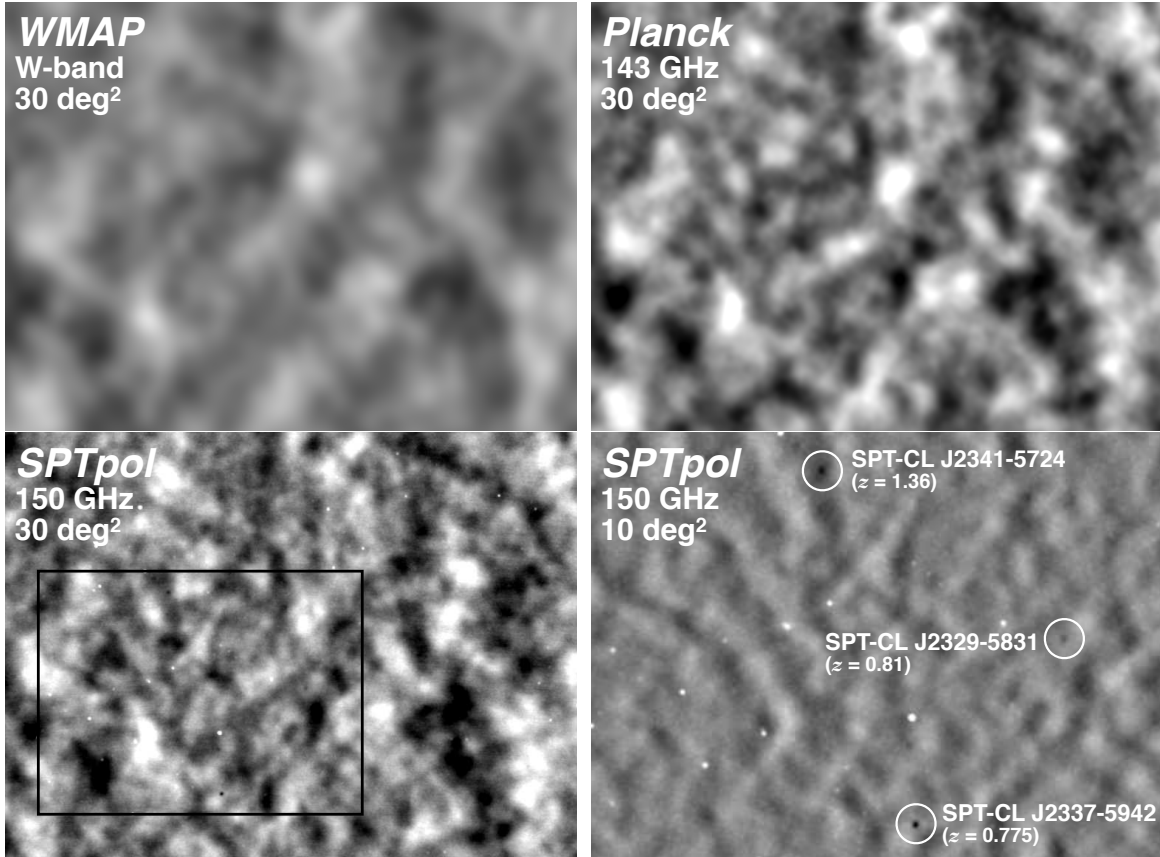[*]Here K$_{\mathrm{CMB}}$ refers to equivalent fluctuation in the CMB temperature, i.e., the temperature fluctuation of a 2.73 K blackbody.

Figure 1. A typical ∼30 deg² field from the SPT-POL survey. *Top*: WMAP *W*-band (*Left*) and *Planck* 143 GHz (*Right*) data from the same region, high-pass filtered at $\ell \sim 50$, for comparison. The large-scale CMB features are measured with high fidelity in both the WMAP, *Planck*, and SPT-POL maps. *Bottom Left*: Minimally filtered SPT-POL data, showing degree-scale and larger structure in the primordial CMB as well as small-scale features such as emissive sources and SZ decrements from galaxy clusters. *Bottom Right*: Zoomed-in view of spatially filtered SPT-POL data indicated by black square in the bottom left panel. In this single 10 deg² region, we indicate three newly SPT-discovered clusters at redshift $z > 0.75$.

## 2. SCIENCE GOALS

The next frontier of CMB research is to extract the wealth of cosmological information available from its polarization, in particular with regards to cosmic inflation and neutrinos .[23,24] The current generation of CMB polarization experiments use a variety of experimental approaches. For example, BICEP2/KECK,[25,26] a pair of ground-based instruments taking data at the South Pole, have ∼1-degree resolution and high raw sensitivity in a single 150 GHz band; ABS[27] is an instrument with similar design philosophy currently being deployed in Chile; and the balloon-borne SPIDER project,[28] with similar angular resolution, but with more observing bands and drastically reduced atmospheric contamination compared to ground-based observatories, is expected to take its first flight in the 2014-2015 Austral summer. These instruments are efficiently designed to focus on measuring the tensor-to-scalar ratio $r$ (and, hence, the energy scale of inflation), but they will have little or no sensitivity to small-scale temperature and polarization. Planned upgrades and observations with the balloon-borne EBEX[29] and ground-based ACT[30] and POLARBEAR[31] experiments will, by contrast, have sufficient resolution to measure smaller-scale signals—at the cost of added complexity in instrument and optics design.

The low-resolution, single-band approach was appropriate for a pathfinding mission in the era in which no *B*-mode polarization was detected, and indeed this approach may have resulted in the first successful detection of *B* modes from inflation .[32] However, if the goal is full characterization of the inflationary and lensing *B*-mode signals (and the *E*-mode spectrum), there are several advantages afforded by a large telescope aperture and

| Experiment | $N_{bolo}$ | $NET_T$ ($\mu K\sqrt{s}$) | $Speed_T$ | $NET_P$ ($\mu K\sqrt{s}$) | $Speed_P$ |
|---|---|---|---|---|---|
| SPT-SZ | 960 | 22 | 1.0 | - | - |
| SPT-POL | 1,536 | 14 | 2.5 | 20 | 1.0 |
| SPT-3G | **15,234** | **3.4** | **43** | **4.8** | **17** |

Table 1. The number of bolometers, sensitivity, and relative mapping speed of SPT-SZ, SPT-POL, and SPT-3G. The sensitivity is quoted as noise-equivalent-temperature (NET) in CMB units for temperature (T) and polarization (P).

multi-band observation. First, the scope of science that can be targeted with a high-resolution, multifrequency instrument is far broader: CMB lensing (only measurable on small angular scales) promises both significant improvements in cosmological constraints and an opportunity to correlate tracers of structure with the underlying matter field; fine-scale $E$-mode polarization can greatly increase science yield from the CMB damping tail; small-scale temperature anisotropy measurements can provide information about the epoch of reionization, but only if multiple bands are used to tease apart the SZ and foreground signals; and measurements of galaxy clusters can inform models of dark energy and gravity (again, only if different signals can be distinguished spectrally). Second, a high signal-to-noise map of the lensed $B$ modes can be used with the measured $E$ modes to reconstruct the lensing potential and separate the lensing $B$-mode signal from the inflationary signal, thus improving the constraints on $r$ and the shape of the tensor spectrum —a process often referred to as "delensing".[33,34] Finally, many instrumental polarization systematics—particularly those having to do with beam mismatch—that can contaminate low-$\ell$ $B$ modes for experiments with large beams, are drastically reduced in high-resolution measurements .[35]

Beyond resolution and frequency coverage, realizing the ambitious goals of exploring the neutrino mass scale, delensing for inflationary $B$-mode searches, and exploiting the full scientific yield of small-scale CMB temperature measurements requires a major leap in observing power. For example, the ability to delens is a strong function of instrument resolution and map noise, and significant delensing is only possible with a $\lesssim 10'$ beam and $\lesssim 5$ $\mu$K-arcmin noise in the $B$-mode map.[33] Similarly, data from neutrino oscillation experiments require that the sum of the neutrino masses be $\Sigma m_\nu \geq 0.05$ eV, although the true value of $\Sigma m_\nu$ will depend on the ordering of the three masses—the so-called "mass hierarchy". In the "inverted hierarchy" scenario, there are two neutrinos with $m_\nu \geq 0.05$ eV and thus $\Sigma m_\nu \geq 0.1$ eV. The limit on $\Sigma m_\nu$ from *Planck* alone is expected to be just above this threshold; however, the combination of *Planck* and an experiment with $\lesssim 5$ $\mu$K-arcmin noise (in $E$ and $B$, and $\sqrt{2}$ lower in $T$) over at least 1000 deg$^2$ would drive this limit closer to 0.05 eV, a regime in which the mass hierarchy can be directly addressed. To map $\geq$1000 deg$^2$ to this noise level requires an order of magnitude improvement in mapping speed over SPT-POL.

The SPT-3G instrument will deliver this with an unprecedented combination of sensitivity and resolution. With ~1' beams, a combined focal plane sensitivity of ~4.8 $\mu K\sqrt{s}$ in polarization, and 24-hour access to clean patches of nearly foreground-free sky from one of the best available sites on Earth for mm-wavelength observations, SPT-3G should achieve a $B$-mode noise level of ~3.5$\mu$K-arcmin, enabling the production of high signal-to-noise images of the lensing $B$ modes. Combined with data from *Planck* and BOSS, SPT-3G will achieve $\sigma(\Sigma m_\nu)$~0.06 eV. Combined with SPT-3G's exquisite $E$-mode measurement, the lensing $B$ mode measurement will allow delensing of the primordial gravitational-wave $B$-mode signal with a factor of 4 reduction in power.[33] This delensing ability will enhance SPT-3G's own constraint on $r$ and naturally complement the KECK program, which is observing the same region of sky. The measurement of small-scale temperature anisotropy from such a survey will provide exciting new constraints on the epoch of reionization. Additional science from SPT-3G will be significantly enhanced by the synergy with the deep and wide optical survey, DES, which will cover the full SPT-3G footprint: 1) The SPT-3G CMB lensing data will be used to produce maps of the projected mass between us and the CMB last scattering surface. These mass maps can be correlated with tracers of large-scale structure, such as optically selected galaxies, effectively allowing us to "weigh" the galaxies. 2) The differential kinetic SZ signal from pairs of galaxy clusters identified in DES data will provide a unique test of General Relativity on ~200 Mpc scales. 3) Both the temperature and polarization information will further improve constraints on cosmology from the SPT-3G and DES galaxy cluster samples, particularly by sharpening the mass-observable calibration with CMB-cluster lensing. Finally, as with SPT-SZ and SPT-POL, the data from SPT-3G will be released to the community to enhance its scientific impact.
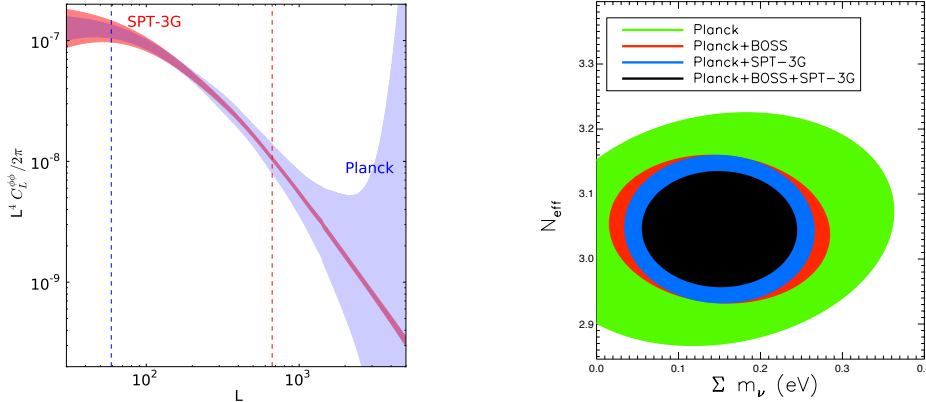
Figure 2. *Left:* Projected error bars (per logarithmic bin size of d(ln$\ell$=0.1)) on the CMB lensing power spectrum for SPT-3G (red) and *Planck* (blue). Dashed vertical lines show the scale at which mapping of individual modes will be possible for *Planck* (blue) and SPT-3G (red). *Right:* Projected 1$\sigma$ parameter constraints on $\Sigma m_\nu$, the sum of the neutrino masses and $N_{\text{eff}}$, the effective number of neutrino species for SPT-3G when combined with data from *Planck* and the BOSS spectroscopic survey. The addition of the extremely deep CMB polarization and lensing maps from SPT-3G will substantially improve cosmological constraints on neutrino physics, including the sum of the masses and the number of relativistic species.

In the following sections, we present projected results from SPT-3G, including cosmological parameter constraints, in each of these areas of research. We assume a four-year survey over 2500 deg$^2$ and the focal plane specifications outlined in Section 3.3 and Table 1. Assuming a 25% observing duty cycle (conservative compared to the 60% efficiency achieved during winter months with SPT-SZ), this results in predicted map noise levels of $\sim$3.5$\mu$K-arcmin in $E$ and $B$ at 150 GHz ($\sqrt{2}$ lower in $T$) and $\sim$6$\mu$K-arcmin in $E$ and $B$ at 95 and 220 GHz. The choice of observing region size and location (2500 deg$^2$ roughly covering the footprint of the original SPT-SZ survey) is motivated by achievable depth and predicted foreground levels, which drive us to smaller observing area, and the constraint on $\Sigma m_\nu$ and the synergy with DES, which drive us to larger area.

## 2.1 CMB Lensing

The SPT-3G CMB lensing measurements will significantly improve the imaging of matter fluctuations between us and the CMB surface of last scattering on small angular scales. This will lead to both a detailed measurement of the lensing power spectrum and a high signal-to-noise map of the projected mass in the Universe. As shown in Figure 2, the combination of improved map noise and resolution compared to *Planck* will result in an SPT-3G map of projected matter fluctuations with high signal-to-noise on scales larger than $\sim$15$'$ ($\ell \lesssim 750$), and SPT-3G will measure the power spectrum of the lensing potential at high significance out to $\ell \approx 5000$. This precise measurement of the growth of structure leads to strong constraints on cosmological parameters. Table 2 shows the combined parameter constraints from CMB lensing and primordial power spectrum constraints (see Section 2.2), and constraints on one key parameter combination are shown in Figure 2. Significant improvements over *Planck* alone are seen in many parameters, particularly in the neutrino sector. SPT-3G+*Planck* will place stringent constraints on the number of relativistic species at recombination and thus confirm or rule out the hints of a fourth neutrino species from CMB and direct neutrino measurements.[34] The combined sensitivity to $\Sigma m_\nu$ will be $\sigma(\Sigma m_\nu) \sim 0.06$ eV, which is roughly six times better than future beta decay experiments such as KATRIN[36] and comparable to the largest neutrino mass splitting. At this level of precision, SPT-3G will either measure $\Sigma m_\nu$ and determine the mass scale for neutrinos, or will place strong pressure on an inverted neutrino mass hierarchy. A yet tighter limit is achievable: if we assume the standard number of neutrinos and a perfect measurement of $H_0$, the constraint on $\Sigma m_\nu$ improves to $\sigma(\Sigma m_\nu) = 0.018$ eV.

Additionally, the high signal-to-noise projected mass map can be cross-correlated with other probes of large scale structure to measure the bias of these tracers to better than 1%, providing new clues on the link between galaxies and dark matter halos. This large area mass map will be extremely useful for comparisons with cosmic

| Dataset | $\sigma(\Omega_b h^2)$ $\times 10^4$ | $\sigma(\Omega_c h^2)$ $\times 10^3$ | $\sigma(A_s)$ $\times 10^{11}$ | $\sigma(n_s)$ $\times 10^3$ | $\sigma(h)$ $\times 10^2$ | $\sigma(\tau)$ $\times 10^3$ | $\sigma(N_{\text{eff}})$ $\times 10^1$ | $\sigma(\Sigma m_\nu)$ [meV] | $\sigma(r)$ $\times 10^2$ |
|---|---|---|---|---|---|---|---|---|---|
| | | | | Cosmological parameter constraints | | | | | |
| *Planck* | 1.93 | 2.02 | 5.36 | 7.07 | 1.88 | 4.96 | 1.39 | 117 | 5.72 |
| + SPT-POL | 1.64 | 1.71 | 4.92 | 6.19 | 1.58 | 4.95 | 1.17 | 96 | **2.75** |
| + SPT-3G | **1.02** | **1.25** | **4.18** | **4.61** | **1.14** | 4.94 | **0.76** | **74** | **1.05** |
| *Planck* + BOSS | 1.34 | 1.21 | 4.01 | 4.54 | 1.21 | 4.92 | 0.74 | 88 | 5.72 |
| + SPT-3G | **0.85** | **0.95** | **3.71** | 3.91 | **0.94** | 4.90 | **0.58** | **61** | **1.05** |

Table 2. Expected $1\sigma$ constraints on cosmological parameters using SPT-3G power spectrum and lensing reconstruction data, assuming a 9-parameter $\Lambda$CDM+$N_{\text{eff}}$+$\Sigma m_\nu$+tensor model. Parameters for which adding SPT-3G improves the constraint by at least a factor of 1.5 over the *Planck* or *Planck*+BOSS constraint are marked in **blue**, while those for which the constraints improve by at least a factor of 1.25 are marked in **orange**.

shear measurements using galaxies, both as a high-redshift complement allowing reconstruction of mass fluctuations that are beyond the reach of these surveys, and as a valuable cross-check and calibration for lower redshift structures that are measured in common.

## 2.2 Primordial CMB Polarization

The high signal-to-noise lensing $B$-mode measurement discussed in the previous section, combined with an ultra-high-fidelity $E$ mode measurement (see Figure 3), will allow us to reduce the lensing contribution to the large-scale $B$ modes in SPT-3G data by a factor of 4. The raw statistical power of the proposed SPT-3G survey is such that this delensing would enable an extremely tight constraint on $r$ ($\sigma(r) \ll 0.01$). Of course, raw sensitivity will not be the limit to the SPT-3G measurement of $r$. Foreground contamination is mitigated by the choice of observing region and bands: the $2500\,\text{deg}^2$ region chosen for the survey has diffuse dust levels within a factor of 1.5 of the best $500\,\text{deg}^2$ of sky being targeted by SPT-POL and the KECK array, and foreground power can be strongly suppressed by making linear combinations of the three observing bands. At the focal plane sensitivity level that SPT-3G is targeting, atmosphere may become an issue, even for polarization measurements and considering the exceptionally low level of atmospheric fluctuation power at the South Pole. The SPT-3G detector design, with matched bolometers measuring orthogonal polarizations in a single pixel, should be extremely efficient in differencing out the atmosphere. In SPT-SZ data, we can difference neighboring detectors with no attempt at gain matching and achieve nearly a factor of 100 in suppressing the common-mode atmospheric signal; for the purposes of forecasting here, we make the conservative assumption that including the differencing of orthogonal polarizations in each pixel, SPT-3G will achieve a factor of 200 common-mode rejection (Note, the intrinsic polarization of the atmosphere has been limited to be less than $10^{-3}$ above the Antarctic Plateau[37]). Figure 3 shows the projected $EE$ and $BB$ constraints using these assumptions about noise, foregrounds, atmosphere, and delensing as well as conservative assumptions for bolometer/readout $1/f$ noise and realistic $E$-$B$ separation appropriate for a Monte-Carlo "pseudo-$C_\ell$" analysis pipeline. These $BB$ error bars would result in a constraint on the tensor-to-scalar ratio of $\sigma(r) = 0.010$, or a 95%-confidence upper limit of $r < 0.021$ for no detection.

In addition to the high level of foreground and atmospheric mitigation, and the systematic advantages of a large telescope aperture, the SPT-3G design addresses other potential sources of systematic error that could limit the constraint on $r$. Concerns about large-scale ground contamination are addressed by a carefully modeled and constructed shielding system. The polar location of the telescope and the default raster scanning strategy present no barriers to low-$\ell$ sensitivity, as demonstrated theoretically[38] and in practice.[32,39] In addition, the SPT-3G survey data would contribute significantly to the measurement of $r$ through synergy with the KECK array data. Delensing by a factor of 4 using SPT-3G data would allow the KECK team to use data in an $\ell$ range where it would normally be dominated by the lensing signal, potentially significantly improving the constraint on $r$ and the shape of the tensor spectrum. This is only possible for datasets that observe the same part of the sky, so SPT-3G is in a unique position to deliver this improvement for KECK.

Finally, the extremely high-fidelity measurement of the $E$-mode polarization of the CMB will yield scientific bounty beyond just the delensing of the primordial $B$ modes. Measurements of the $E$-mode damping tail are expected to become foreground-limited at much higher $\ell$ than the temperature damping tail, because of the expected low polarization of dusty point sources.[41] This allows a low-noise, high-resolution experiment such as
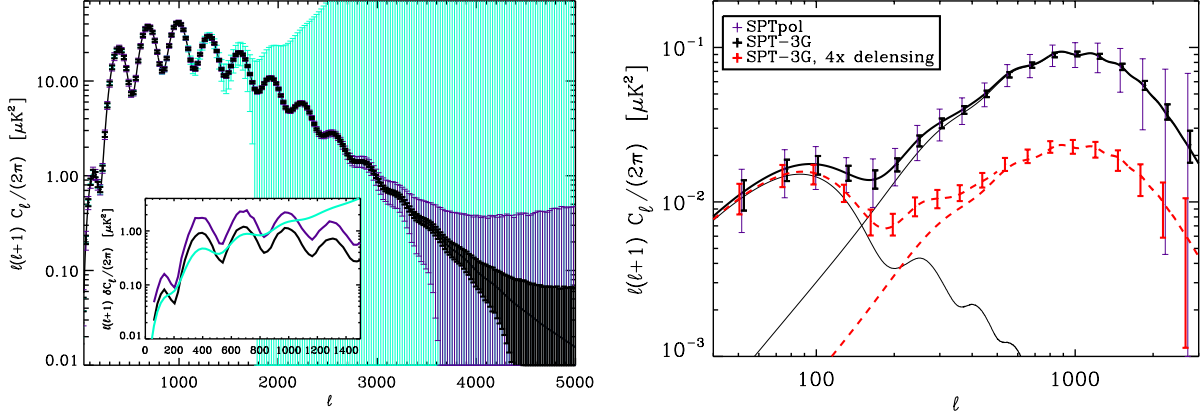
Figure 3. Projected $EE$ (left) and $BB$ (right) constraints from four years of observing with the SPT-3G camera (black points and error bars). Constraints are from simulated observations including realistic treatment of foregrounds, atmosphere, instrument $1/f$ noise, and $E$-$B$ separation. Overplotted are projected constraints from $Planck$[40] (cyan) and SPT-POL (purple). The inset in the $EE$ plot shows the amplitude of the low-$\ell$ $EE$ uncertainties from the three instruments (same color scheme), showing that SPT-3G is competitive with $Planck$'s low-$\ell$ $EE$ constraints down to $\ell \sim 200$. Model curves in the $BB$ plot (solid lines) are for $\Sigma m_\nu = 0$, with $r = 0$ and $r = 0.2$. The red points and dashed lines in the $BB$ plot show the added sensitivity to primordial gravitational-wave $B$ modes from delensing. The SPT-3G error bars are recalculated for a 4 reduction in lensed $BB$ power, and the model lines are shown with this reduction for the same models as the solid lines in the main plot.

SPT-3G to extract information from the $E$-mode damping tail out to very high $\ell$, with the potential for precision measurements of the number of relativistic particle species, the primordial helium abundance, and the running of the scalar spectral index.

## 2.3 Epoch of Reionization

The epoch of reionization is the second major phase transition of gas in the Universe (the first being recombination). Reionization occurs comparatively recently, $z \sim 10$ instead of 1100, and marks a milestone in cosmological structure formation. It begins with the creation of the first objects massive enough to produce a significant flux of UV photons (e.g., stars). We expect ionized bubbles to form around the initial UV sources with these HII bubbles eventually merging to produce the completely ionized Universe we see today. Observing the $z \sim 10$ Universe is extremely challenging, and as a result we know very little about the epoch of reionization. From studies of the Lyman-$\alpha$ forest, we know that the Universe is ionized by $z \sim 6$, with some (as yet inconclusive) evidence for a decreasing ionization fraction at $z > 6$. Studies of 21 cm emission have also excluded instantaneous reionization models ($\Delta z < 0.06$).

The kinetic SZ (kSZ) effect provides a unique means to study reionization. The kSZ effect occurs when CMB photons are Doppler shifted by the bulk motion of electrons, leading to a small change in the blackbody temperature of the CMB. Reionization should produce a significant kSZ signal due to the huge contrast in the free electron density between neutral and ionized regions. The angular frequency dependence of the kSZ signal encodes information on the bubble size and therefore the typical energy of an ionizing source. The amplitude of the kSZ power is roughly proportional to the number of bubbles and therefore the duration of reionization. We can combine the duration of reionization derived from the kSZ with timing information from other probes, such as the integrated optical depth from large-scale CMB polarization measurements or the first 21 cm detections, to constrain the ionization history of the Universe.

The sensitivity of SPT-3G will be sufficient to robustly detect the kSZ power with a $1\,\sigma$ uncertainty of $0.125\,\mu\text{K}^2$. This detection would translate into a $1\sigma$ constraint of $\sigma(\delta z) \sim 0.25$ on the duration of the epoch of reionization. Combining the strong constraints on the total optical depth from $Planck$ with SPT-3G's measurement of the duration would tightly constrain the evolution of the ionization fraction and would rule out or confirm at high significance models with reionization ending near $z = 6$.
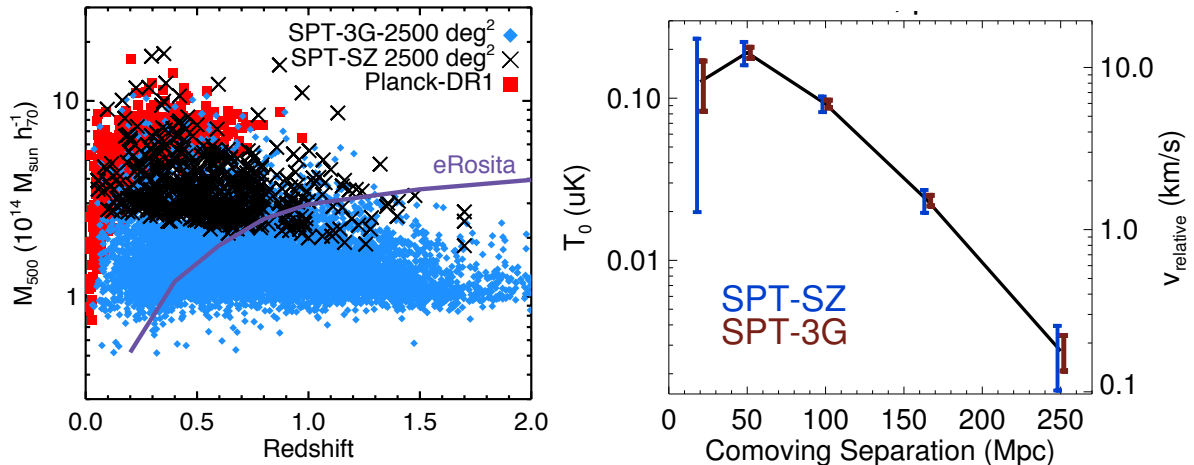
Figure 4. (Left) Mass versus redshift for three cluster samples: (1) SZ-selected clusters from 2500 deg$^2$ of the SPT-SZ survey,[8] (2) SZ-selected clusters from the *Planck* survey, and (3) the projected SPT-3G cluster sample. Also over-plotted is the expected selection threshold from the upcoming eRosita X-ray cluster survey.[42] (Right) Projected measurement by SPT-SZ and SPT-3G of the relative velocities of pairs of DES-selected clusters using the kinetic SZ effect,[43] a unique probe of gravity on scales of 100s of Mpc. SPT-3G is expected to provide a $30\sigma$ detection significance using the DES cluster sample with photometric redshifts.

## 2.4 Cluster Science

Clusters of galaxies are the largest gravitationally bound objects in the Universe. Their large masses make them a unique cosmological probe sensitive to gravity and the growth of structure on the largest physical scales. As demonstrated by SPT-SZ, a high-resolution SZ cluster survey can uniquely find the most massive clusters in the Universe nearly independently of redshift. SPT-3G will extend the work of SPT-SZ by covering a nearly identical survey area with noise levels $\sim$12, 7, and 20 times lower at 95, 150, and 220 GHz, respectively. This will lower the cluster mass threshold and therefore extend the redshift reach of SPT-3G, allowing it to find an order of magnitude more clusters, and, in combination with the DES cluster survey, improved dark energy constraints.

In Figure 4, we show the projected mass and redshift distribution for the SPT-3G cluster catalog, compared to the SZ-selected catalogs from SPT-SZ [8] and *Planck*.[44] SPT's smaller beam allows it to find higher redshift clusters than *Planck*. Relative to SPT-SZ, the deeper SPT-3G data will find more clusters and extend to higher redshift, opening a new window into an earlier epoch of cluster formation. We project that SPT-3G will find $\sim$5000 clusters at a signal-to-noise $> 4.5$, corresponding to a 97% purity threshold. The SPT-3G survey will strongly complement the DES cluster survey, which is expected to find tens of thousands of clusters at $z \lesssim 1$. The SZ data effectively provides a calibration of the scatter in the DES richness-mass relation. Such a calibration is predicted to increase the dark energy figure-of-merit by a factor of several.[45] With improved calibration of the DES richness-mass relation, the DES cluster survey is predicted to have a dark energy FOM of $\sim$100.[46] DES, in combination with the VISTA survey, will also measure photometric redshifts for the SPT-3G clusters at $z \lesssim 1$, which includes $\sim$75% of the SPT-3G sample, with higher redshift clusters requiring separate follow-up with optical and near-infrared imagers on larger telescopes (e.g., Magellan/FourStar, Gemini/F2, SOAR/Spartan).

The deep SPT-3G maps are essential to enable the detection and utility of CMB-cluster lensing, a signal that has yet to be measured. On an individual cluster basis, SPT-3G will measure CMB-cluster lensing with signal-to-noise of $\sim$1 for the most massive clusters.[47] For the ensemble of 5000 SPT-3G-selected clusters, we expect to provide an absolute mass calibration with 3-5% accuracy using quadratic estimators of the cluster lensing signal,[48] using either temperature or polarization information. This is comparable to the predicted statistical precision (2%) of the stacked optical weak lensing for DES.[46] The CMB-cluster lensing mass calibration would be an important systematic check of the stacked weak lensing mass-calibration, especially at high redshift, because of the CMB's well characterized statistical properties and high, but known, redshift.

## 2.5 A Test of General Relativity on ∼200 Mpc Length Scales

With SPT-3G we will be able to perform the most direct test yet of the gravitational force law on large (∼200 Mpc) scales. General Relativity leads to precise predictions of the tendency of one galaxy cluster to fall toward another, which generates a differential Doppler shifting of CMB photons as they scatter off the electrons in each cluster's intracluster plasma. While this "pairwise kSZ" signal is small, it was recently detected at the $3\sigma$ level in ACT data[49] by stacking many pairs of galaxy clusters. We forecast that SPT-3G will detect this signal with $30\sigma$ significance using the DES cluster sample with realistic photometric redshifts,[43] as shown in Figure 4. This is effectively a ∼3% measurement of the strength of gravity on ∼200 Mpc scales. A spectroscopic survey of the DES clusters would strengthen this test, particularly on <100 Mpc scales, resulting in a > $40\sigma$ detection. We will either achieve a high-precision verification of General Relativity on large scales, or discover a breakdown of the theory's predictive power. The latter would almost certainly be treated as a very important clue about the physics driving cosmic acceleration.

# 3. INSTRUMENT

The SPT-3G instrument design combines new optics, cryostat, detectors, and readout to achieve a factor-of-20 increase in mapping speed over SPT-POL. A new secondary mirror and cold tertiary optics will increase the optical throughput by greater than a factor of two; new multi-chroic detector arrays in the larger focal plane area will increase the detector count by an order of magnitude, and a new readout will increase the multiplexing factor by a factor of four.

A focal plane array of multi-chroic pixels offers several advantages over an array of single-band pixels. The optics, lens anti-reflection (AR) coatings and pixel diameter are all optimized for 150 GHz mapping speed—nearly equivalent to the performance of an optimally configured single-band 150 GHz array using the entire available focal plane area. The additional 95 and 220 GHz bands enabled by the multi-chroic pixels achieve 69% and 54% of the optimal single-frequency mapping speed, respectively, accounting for both the sub-optimal pixel size and AR coating reflection losses.

## 3.1 Optical Design

The SPT-3G optical design uses an ambient temperature secondary mirror coupled to a system of cryogenic lenses to provide a much wider field of view than the current SPT configuration, see Figure 5. Through the use of a cold Lyot stop, we expect to achieve greater systematic control of stray light, lower instrumental optical loading on the detectors, and thus greater sensitivity per detector.

The optical design employs an ellipsoidal secondary mirror tilted at the Dragone angle to eliminate cross-polarization at the center of the image plane. A flat tertiary mirror sends the light to three cryogenic alumina lenses, which reimage the Gregorian focus and form a cold aperture stop. The 430-mm diameter $f/1.83$ image plane covers a 1.9° field of view (FOV), or 2.8 square degrees, and is matched to the size of the tiled focal plane array of 2539 lenslet coupled pixels described in Section 3.3. The optical performance is excellent, with Strehl ratios > 0.98, 0.96, and 0.93 at 95, 150, and 220 GHz, respectively, across the FOV. With this image plane focal ratio, the hex-close-packed array of 6-mm diameter lenslets provides nearly optimal mapping speed in the 150 GHz band.

The alumina lenses are single-convex conic shapes to keep the optical design simple and to facilitate manufacture and antireflection coating. Each lens is 720 mm diameter and between 51-65 mm thick, which conforms to the manufacturing limit of our alumina vendor.[†] Using a sample of 99.5% purity alumina provided by the vendor, we have measured a warm index of refraction of $n = 3.12\pm0.01$ and a 120 K loss tangent of $\tan\delta = 0.9\pm0.2\times10^{-4}$. The total attenuation through the three lenses is 10%, 14%, and 19% at 95, 150, and 220 GHz, respectively.

To address the broadband anti-reflection requirements of the large alumina lenses (and the silicon focal plane lenslets described in section 3.3), we have developed coating materials which can be adjusted to achieve a wide range of dielectric constants (see Figure 6). The materials are made from mixtures of different epoxy-bases as well as a high-dielectric constant additive that can be molded or machined after curing to the appropriate

---

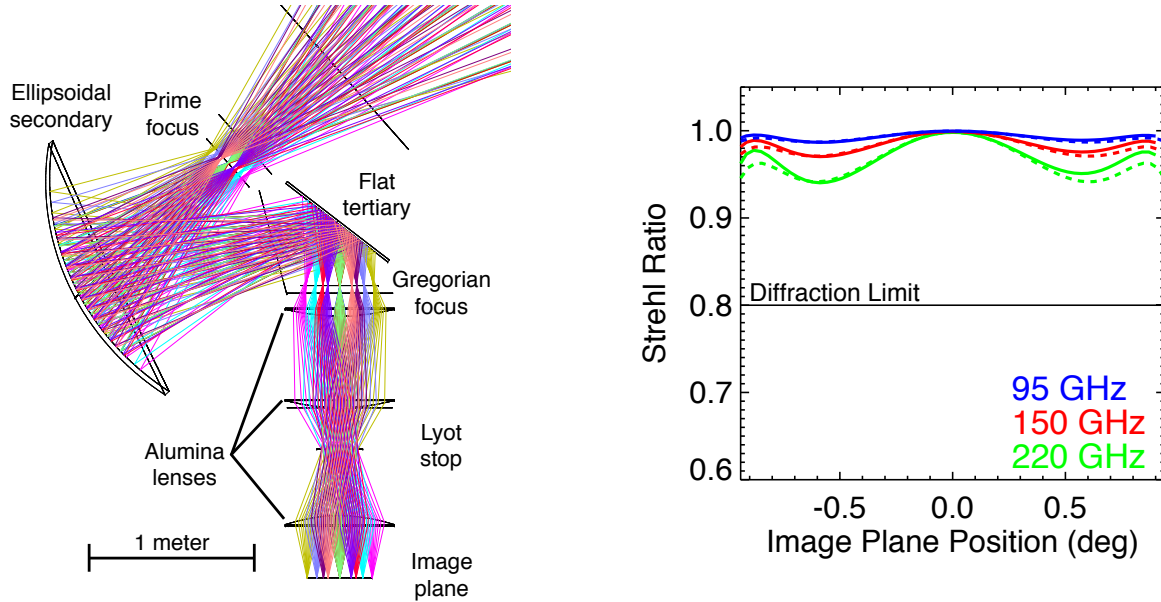[†]CoorsTek, http://www.coorstek.com/

Figure 5. *Left:* Layout of the SPT-3G optical design. The optics consist of an ellipsoidal secondary mirror and three cryogenically cooled alumina lenses. A cold Lyot stop defines the 8 m primary illumination and controls stray light. *Right:* Strehl ratio vs focal plane position at 95 (blue), 150 (red), and 220 (green) GHz. The lines corresponds to a cut across the focal plane's y-axis (solid) and x-axis (dashed). The 430 mm diameter focal plane covers a 1.9° FOV at with $f/1.83$ beams. The optical performance is excellent, with Strehl ratios $> 0.98, 0.96, 0.93$ at 95, 150, 220 GHz, respectively, across the FOV.

thickness. Prototype flats and lenslets with multiple, tuned dielectric constant layers have been fabricated, survived many cryogenic thermal cycles, and shown to perform well optically over a broad band (see Figure 6). The total reflection losses for a preliminary 3-layer coating design formed from these materials and optimized at 150 GHz, over 7 surfaces (three lenses plus the silicon lenslet), are calculated to be $6\%, 3\%,$ and $17\%$ at 95, 150, and 220 GHz, respectively.

### 3.2 Receiver Design and Cryogenics

The SPT-3G receiver design builds upon the tested technology of SPT-SZ and SPT-POL. The focal plane is cooled to $\sim 260$ mK by a $^3$He-based closed cycle refrigerator [‡], operating from a Cryomech pulse-tube cryorefrigerator. The $^3$He refrigerator will be three-stage $^4$He-$^3$He-$^3$He system, similar to what was used for both SPT-SZ and SPT-POL, except with an additional head for the $^4$He stage, designed to provide an additional thermal intercept to buffer the $^3$He stages and increase the receiver duty cycle to $> 90\%$. The cold optics share a common vacuum space with the focal plane, but are cooled by their own pulse-tube refrigerator to simplify the cryogenic design as well as increase overall cooling power.

The large optical throughput of the instrument requires a 700-mm diameter vacuum window located at the Gregorian focus. An expanded polyethylene foam window provides both thermal insulation and IR blocking. To achieve this large diameter, we plan to mechanically support the cold side of the foam using the first alumina lens. FEA analysis of the alumina indicates that it has sufficient strength to perform this role. The window supporting lens will be conductively cooled to $< 70$ K using the first stage of the optics pulse-tube cooler. This has the benefit of reducing mm-wavelength emission and IR loading on the 4 K optics, will reduce the number of free-space capacitive mesh filters needed, and will result in much lower total mm-wave emission on the focal plane than in the current generation SPT receiver. A smaller prototype foam window with a cooled back surface has already been built and demonstrated by UC-Berkeley.

---

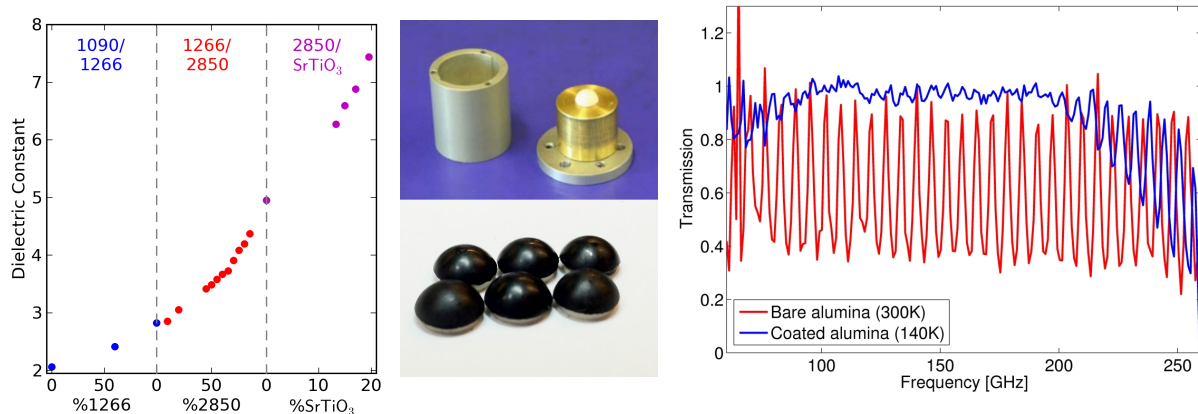[‡] Chase Research, http://www.chasecryogenics.com/

Figure 6. *Left:* Measured dielectric constants of three different combinations of moldable epoxies and high-dielectric-constant fillers in varying ratios. The label at the top indicates the type of epoxy or dielectric filler used. The range of values needed for broadband anti-reflection coating for the full frequency range of 95, 150, and 220 GHz has been achieved. *Center:* Photo of an alumina test lenslet installed in a two-piece molding jig and six lenslets with completed two-layer molded anti-reflection coatings. *Right:* Measured transmission through alumina test flat with two-layer filled/unfilled epoxy anti-reflection coating on both sides. SPT-3G will use three-layers to extend the bandwidth across its 220 GHz band.

The second and third lenses and the 300 mm Lyot stop are cooled to $\sim 4\,\mathrm{K}$. At the Lyot stop, blocking filters from our collaborators at Cardiff reduce the radiative heat load on the 260 mK stage to an acceptably low level, and similar filters placed at 260 mK ensure no out-of-band blue leaks can couple to the detectors above our 220 GHz band. We calculate that with this cryo-optical design, we will decrease the internal loading from the $\sim 30\,\mathrm{K}$ measured in SPT-SZ at 150 GHz to $\sim 10\,\mathrm{K}$. This, coupled with the slightly increased optical efficiency, will reduce the NET by $\sim 1.4$ and increase the mapping speed per detector by $\sim 2$ relative to SPT-SZ.[2]

### 3.3 Focal Plane Array

The wide-field reimaging optics described above will allow a much larger number of independent pixels in SPT-3G compared to SPT-POL, 2539 vs. 768. Each pixel will have six detectors that measure the polarization in three bands at 95, 150, and 220 GHz, for a total of 15,234 bolometers. The three-band, two-polarization pixel (see Section 3.4) is based on ongoing multi-chroic detector development at UC-Berkeley and Argonne National Labs (ANL).

The SPT-3G array builds on a design successfully utilized in the POLARBEAR-1 experiment (see Fig. 7). The SPT-3G array consists of seven hexagonal modules surrounded by twelve partial modules which together fill the 430 mm diameter focal plane. Each full module has 217 pixels with detectors fabricated from a single 6 inch silicon wafer. The 6 inch wafer processing has been prototyped at UC-Berkeley. Wiring is routed out the back of the focal plane via flexible superconducting ribbon cables, as in SPT-POL, with the LC filters mounted behind the silicon detector wafers as shown in Figure 7.

### 3.4 Three-band pixel

The multi-chroic pixel of SPT-3G uses a two-octave bandwidth log-periodic "sinuous" planar antenna coupled to a 6 mm diameter silicon lens. The silicon lenslets provide an excellent index match to the wafer, and will be AR-coated using the same three-layer loaded-epoxy technique described above for the alumina lenses in the cold optics. We will mold the AR coatings using a precise metal mold, a process that we have already used for prototypes. The lens-coupled antenna architecture has been used extensively with mm-wave mixers and is currently in use with the HIFI instrument on the *Herschel* spacecraft.[50] The beam pattern of the antenna/lenslet combination is determined by diffraction with an effective aperture that is the size of the lenslet. The lenslets are registered to the antenna using circular depressions that are trench etched into a "spacer" wafer that is in direct contact with the bolometer wafer. The etched depressions are positioned accurately to within several microns and
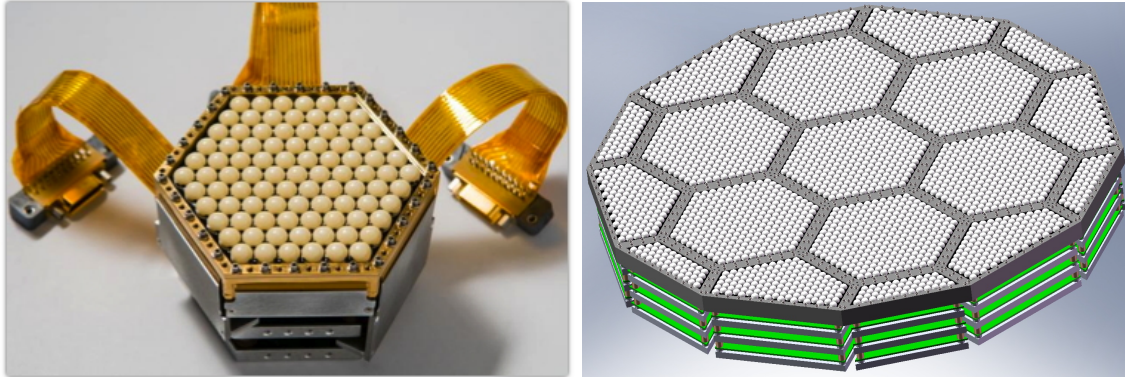
Figure 7. *Left:* Photograph of POLARBEAR-1 91 pixel lens-coupled module. *Right:* CAD drawing of SPT-3G focal plane.
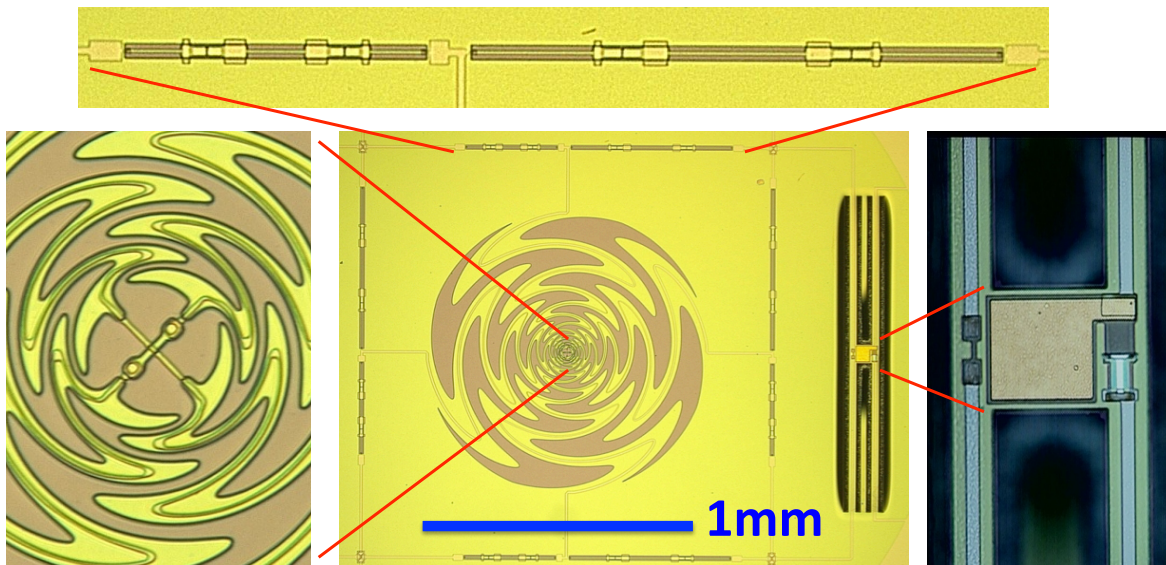


Figure 8. Photographs of a dual-frequency (90/150 GHz) band pixel using a sinuous log-periodic antenna developed at UC-Berkeley. The center picture shows the pixel layout including the antenna, one of the four TES bolometers, and associated microstrip circuitry. All components of a pixel fit within the footprint of a 6 mm lenslet mounted on the reverse side of the wafer. The antenna connects to microstrip transmission lines (inset on left) which run on top of the metal antenna arms using them as a ground plane. The RF signals are split into two bands by lumped diplexing filters (inset on top) and terminate on a thermally isolated TES bolometer island (inset on the right). SPT-3G will use 95/150/220 GHz triplexed pixels.

the spacer wafer and bolometer wafer are aligned optically to the needed accuracy ($< 0.1$ wavelengths). Lenslet-coupled bolometers have been successfully implemented by the POLARBEAR-1 experiment which deployed an array of 1,274 single-color lens-coupled pixels in January 2012 .[51,52] They have demonstrated high end-to-end optical efficiency of 40-50% and symmetric, Gaussian beams.

The SPT-3G antenna has four arms: two opposite arms couple to one linear polarization. The antenna has a "self-complementary" architecture (metal and open areas have the same geometry) resulting in an impedance that is independent of frequency. One complication of this design is that the plane of polarization rotates slightly, periodically with frequency, with a 5 degree amplitude. In a 30% fractional band, however, the rotation averages toward zero and the average polarization angle varies less for different source spectra. The calculated polarization angle change between dust and CMB is 0.2°, which is small enough to not affect dust subtraction for nominal dust levels. Furthermore, the array will be composed of left and right-handed pixels so that the final composite beam on the sky will have no polarization angle offsets between different spectral components.

The two antenna arms associated with each polarization couple to a balanced RF circuit including microstrip
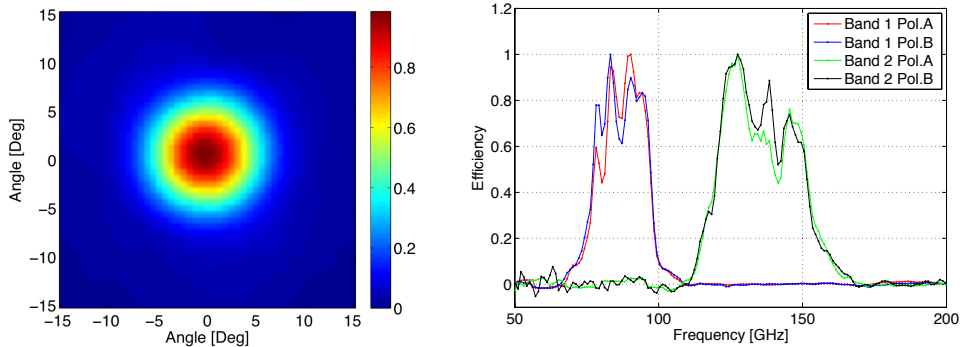
Figure 9. *Left:* Laboratory-measured beam map of sinuous pixel at $\sim 150\,\mathrm{GHz}$. The beam is round, with less than 1% ellipticity. *Right:* Measured spectral response of a prototype dual-band pixel. The plot is normalized to unity, but the efficiency of the receiver is 40-50% implying a pixel efficiency of $\sim 70\%$. The efficiency and bandwidth of the detectors is consistent with designed values. A 95/150/220 GHz triplexed pixel is planned for SPT-3G.

transmission lines from the center of the antenna, triplexer RF filters that route the power from each band into its own microstrip, and finally a termination resistor on each detector. The microstrip transmission lines lie on top of the metal arms of the antenna and use them as ground planes. The filters are composed of lumped elements which have the advantage of being physically compact.

The SPT-3G pixel design is a straightforward extension of ongoing work at UC-Berkeley to develop multichroic pixels with two, three, and seven bands.[53] Figure 8 shows a photograph of a prototype two-band pixel, and Figure 9 shows the associated bandpass and beam measurements.

## 3.5 Readout System

The multiplexed readout system for SPT-3G is based on the digital implementation of the frequency domain SQUID multiplexer (DfMUX) technology[54,55] currently used by SPT-POL, POLARBEAR, and EBEX. We have already demonstrated nominal detector noise (including low frequency performance), robust detector and SQUID setup, and the expected cryogenic wiring heat loads using this system in SPT-POL. For SPT-3G, the increase in detector number requires an increase in multiplexing factor, the number of detectors read out per SQUID, from the presently achieved 16 to 64.

The DfMUX readout system generates a sinusoidal voltage bias carrier for each detector from a Field Programmable Gate Array (FPGA), responsible for one module of 64 detectors. Each detector operates in series with an inductor-capacitor LC resonator, and encodes the sky signal as an amplitude modulation of its bias carrier. The carrier signals from each module of detectors are added together and amplified by a SQUID before being digitized and sent back to the FPGA. The FPGA demodulates each sky-signal encoded carrier separately, and writes the information to disk. The readout system also provides the SQUID bias currents, and sets the optimal operating points for the detectors and SQUIDs.

The new DfMUX system achieves higher multiplexing factors by replacing the bandwidth-limited analog SQUID flux-locked loop (FLL) with a recently demonstrated[56,57] digital feedback system called Digital Active Nulling (DAN). Rather than operating across the entire SQUID bandwidth, DAN provides feedback only across the limited bandwidth of the detectors. This allows for an order of magnitude higher carrier frequency and much longer lengths for the cryogenic wiring. The new readout system will include new DAN-compatible SQUID controller electronics and a newer generation FPGA circuit board that is capable of handling the signal processing from the higher channel-count.

With 64 channel multiplexing, the SPT-3G DfMUX readout will use a similar number of readout circuit boards (60), occupy the same number of electronics crates (3), and use roughly the same amount of electrical power as the existing SPT-POL system (1.5 kW) for the 15,234 SPT-3G bolometers.

# 4. CONCLUSION

In this work, we describe the science goals and design of SPT-3G, the third-generation camera for the SPT. The SPT-3G experiment will cross the threshold from statistical detection of $B$-mode CMB lensing to imaging the fluctuations at high signal-to-noise—enabling the separation of the lensing and inflationary $B$ modes. This will lead to improved constraints on both the amplitude and shape of the primordial tensor power spectrum, and a constraint on the sum of the neutrino masses of 0.06 eV; a level relevant for exploring the neutrino mass hierarchy. To achieve this will require a factor of $\sim$20 increase in mapping speed beyond the already impressive SPT-POL camera. SPT-3G will accomplish this through a combination of increased field of view from a re-designed optical system, and increased sensitivity per pixel through a multi-chroic detector design. First light for the SPT-3G camera is targeted for January 2016.

# ACKNOWLEDGMENTS

# REFERENCES

[1] Ruhl, J., Ade, P. A. R., Carlstrom, J. E., Cho, H.-M., Crawford, T., Dobbs, M., Greer, C. H., Halverson, N. W., Holzapfel, W. L., Lanting, T. M., Lee, A. T., Lerlinitch, E. M., Leong, J., Lu, W., Lueker, M., Mehl, J., Meyer, S. S., Mohr, J. J., Padin, S., Plagge, T., Pryke, C., Runyan, M. C., Schwan, D., Sharp, M. K., Spieler, H., Staniszewski, Z., and Stark, A. A., "The South Pole Telescope," in [*Proc. SPIE, Vol. 5498, Millimeter and Submillimeter Detectors for Astronomy II*], Zmuidzinas, J., Holland, W. S., and Withington, S., eds., 11–29, SPIE Optical Engineering Press, Bellingham (Oct. 2004).

[2] Carlstrom, J. E., Ade, P. A. R., Aird, K. A., Benson, B. A., Bleem, L. E., Busetti, S., Chang, C. L., Chauvin, E., Cho, H.-M., Crawford, T. M., Crites, A. T., Dobbs, M. A., Halverson, N. W., Heimsath, S., Holzapfel, W. L., Hrubes, J. D., Joy, M., Keisler, R., Lanting, T. M., Lee, A. T., Leitch, E. M., Leong, J., Lu, W., Lueker, M., Luong-van, D., McMahon, J. J., Mehl, J., Meyer, S. S., Mohr, J. J., Montroy, T. E., Padin, S., Plagge, T., Pryke, C., Ruhl, J. E., Schaffer, K. K., Schwan, D., Shirokoff, E., Spieler, H. G., Staniszewski, Z., Stark, A. A., Tucker, C., Vanderlinde, K., Vieira, J. D., and Williamson, R., "The 10 Meter South Pole Telescope," *PASP* **123**, 568–581 (May 2011).

[3] Bussmann, R. S., Holzapfel, W. L., and Kuo, C. L., "Millimeter Wavelength Brightness Fluctuations of the Atmosphere above the South Pole," *ApJ* **622**, 1343–1355 (Apr. 2005).

[4] Radford, S. J. E., "Observing Conditions for Submillimeter Astronomy," in [*Revista Mexicana de Astronomia y Astrofisica Conference Series*], *Revista Mexicana de Astronomia y Astrofisica Conference Series* **41**, 87–90 (Nov. 2011).

[5] Padin, S., Staniszewski, Z., Keisler, R., Joy, M., Stark, A. A., Ade, P. A. R., Aird, K. A., Benson, B. A., Bleem, L. E., Carlstrom, J. E., Chang, C. L., Crawford, T. M., Crites, A. T., Dobbs, M. A., Halverson, N. W., Heimsath, S., Hills, R. E., Holzapfel, W. L., Lawrie, C., Lee, A. T., Leitch, E. M., Leong, J., Lu, W., Lueker, M., McMahon, J. J., Meyer, S. S., Mohr, J. J., Montroy, T. E., Plagge, T., Pryke, C., Ruhl, J. E., Schaffer, K. K., Shirokoff, E., Spieler, H. G., and Vieira, J. D., "South pole telescope optics," *Appl. Opt.* **47**(24), 4418–4428 (2008).

[6] Story, K. T., Reichardt, C. L., Hou, Z., Keisler, R., Aird, K. A., Benson, B. A., Bleem, L. E., Carlstrom, J. E., Chang, C. L., Cho, H.-M., Crawford, T. M., Crites, A. T., de Haan, T., Dobbs, M. A., Dudley, J., Follin, B., George, E. M., Halverson, N. W., Holder, G. P., Holzapfel, W. L., Hoover, S., Hrubes, J. D., Joy, M., Knox, L., Lee, A. T., Leitch, E. M., Lueker, M., Luong-Van, D., McMahon, J. J., Mehl, J., Meyer, S. S., Millea, M., Mohr, J. J., Montroy, T. E., Padin, S., Plagge, T., Pryke, C., Ruhl, J. E., Sayre, J. T., Schaffer, K. K., Shaw, L., Shirokoff, E., Spieler, H. G., Staniszewski, Z., Stark, A. A., van Engelen, A., Vanderlinde, K., Vieira, J. D., Williamson, R., and Zahn, O., "A Measurement of the Cosmic Microwave Background Damping Tail from the 2500-Square-Degree SPT-SZ Survey," *ApJ* **779**, 86 (Dec. 2013).

[7] Austermann, J. E., Aird, K. A., Beall, J. A., Becker, D., Bender, A., Benson, B. A., Bleem, L. E., Britton, J., Carlstrom, J. E., Chang, C. L., Chiang, H. C., Cho, H.-M., Crawford, T. M., Crites, A. T., Datesman, A., de Haan, T., Dobbs, M. A., George, E. M., Halverson, N. W., Harrington, N., Henning, J. W., Hilton, G. C., Holder, G. P., Holzapfel, W. L., Hoover, S., Huang, N., Hubmayr, J., Irwin, K. D., Keisler, R., Kennedy, J., Knox, L., Lee, A. T., Leitch, E., Li, D., Lueker, M., Marrone, D. P., McMahon, J. J., Mehl, J., Meyer, S. S., Montroy, T. E., Natoli, T., Nibarger, J. P., Niemack, M. D., Novosad, V., Padin, S., Pryke, C., Reichardt, C. L., Ruhl, J. E., Saliwanchik, B. R., Sayre, J. T., Schaffer, K. K., Shirokoff, E., Stark, A. A., Story, K., Vanderlinde, K., Vieira, J. D., Wang, G., Williamson, R., Yefremenko, V., Yoon, K. W., and Zahn, O., "SPTpol: an instrument for CMB polarization measurements with the South Pole Telescope," in [*Society of Photo-Optical Instrumentation Engineers (SPIE) Conference Series*], *Society of Photo-Optical Instrumentation Engineers (SPIE) Conference Series* **8452** (Sept. 2012).

[8] Bleem, L. E. and the SPT collaboration, "Galaxy Clusters Discovered via the Sunyaev-Zel'dovich Effect in the 2500-Square-Degree SPT-SZ Survey," *in preparation* (2014).

[9] Staniszewski, Z., Ade, P. A. R., Aird, K. A., Benson, B. A., Bleem, L. E., Carlstrom, J. E., Chang, C. L., Cho, H.-M., Crawford, T. M., Crites, A. T., de Haan, T., Dobbs, M. A., Halverson, N. W., Holder, G. P., Holzapfel, W. L., Hrubes, J. D., Joy, M., Keisler, R., Lanting, T. M., Lee, A. T., Leitch, E. M., Loehr, A., Lueker, M., McMahon, J. J., Mehl, J., Meyer, S. S., Mohr, J. J., Montroy, T. E., Ngeow, C.-C., Padin, S., Plagge, T., Pryke, C., Reichardt, C. L., Ruhl, J. E., Schaffer, K. K., Shaw, L., Shirokoff, E., Spieler, H. G., Stalder, B., Stark, A. A., Vanderlinde, K., Vieira, J. D., Zahn, O., and Zenteno, A., "Galaxy Clusters Discovered with a Sunyaev-Zel'dovich Effect Survey," *ApJ* **701**, 32–41 (Aug. 2009).

[10] Vanderlinde, K., Crawford, T. M., de Haan, T., Dudley, J. P., Shaw, L., Ade, P. A. R., Aird, K. A., Benson, B. A., Bleem, L. E., Brodwin, M., Carlstrom, J. E., Chang, C. L., Crites, A. T., Desai, S., Dobbs, M. A., Foley, R. J., George, E. M., Gladders, M. D., Hall, N. R., Halverson, N. W., High, F. W., Holder, G. P., Holzapfel, W. L., Hrubes, J. D., Joy, M., Keisler, R., Knox, L., Lee, A. T., Leitch, E. M., Loehr, A., Lueker, M., Marrone, D. P., McMahon, J. J., Mehl, J., Meyer, S. S., Mohr, J. J., Montroy, T. E., Ngeow, C., Padin, S., Plagge, T., Pryke, C., Reichardt, C. L., Rest, A., Ruel, J., Ruhl, J. E., Schaffer, K. K., Shirokoff, E., Song, J., Spieler, H. G., Stalder, B., Staniszewski, Z., Stark, A. A., Stubbs, C. W., van Engelen, A., Vieira, J. D., Williamson, R., Yang, Y., Zahn, O., and Zenteno, A., "Galaxy Clusters Selected with the Sunyaev-Zel'dovich Effect from 2008 South Pole Telescope Observations," *ApJ* **722**, 1180–1196 (Oct. 2010).

[11] Williamson, R., Benson, B. A., High, F. W., Vanderlinde, K., Ade, P. A. R., Aird, K. A., Andersson, K., Armstrong, R., Ashby, M. L. N., Bautz, M., Bazin, G., Bertin, E., Bleem, L. E., Bonamente, M., Brodwin, M., Carlstrom, J. E., Chang, C. L., Chapman, S. C., Clocchiatti, A., Crawford, T. M., Crites, A. T., de Haan, T., Desai, S., Dobbs, M. A., Dudley, J. P., Fazio, G. G., Foley, R. J., Forman, W. R., Garmire, G., George, E. M., Gladders, M. D., Gonzalez, A. H., Halverson, N. W., Holder, G. P., Holzapfel, W. L., Hoover, S., Hrubes, J. D., Jones, C., Joy, M., Keisler, R., Knox, L., Lee, A. T., Leitch, E. M., Lueker, M., Luong-Van, D., Marrone, D. P., McMahon, J. J., Mehl, J., Meyer, S. S., Mohr, J. J., Montroy, T. E., Murray, S. S., Padin, S., Plagge, T., Pryke, C., Reichardt, C. L., Rest, A., Ruel, J., Ruhl, J. E., Saliwanchik, B. R., Saro, A., Schaffer, K. K., Shaw, L., Shirokoff, E., Song, J., Spieler, H. G., Stalder, B., Stanford, S. A., Staniszewski, Z., Stark, A. A., Story, K., Stubbs, C. W., Vieira, J. D., Vikhlinin, A., and Zenteno, A., "A Sunyaev-Zel'dovich-selected Sample of the Most Massive Galaxy Clusters in the 2500 deg$^2$ South Pole Telescope Survey," *ApJ* **738**, 139–+ (Sept. 2011).

[12] Benson, B. A., de Haan, T., Dudley, J. P., Reichardt, C. L., Aird, K. A., Andersson, K., Armstrong, R., Ashby, M. L. N., Bautz, M., Bayliss, M., Bazin, G., Bleem, L. E., Brodwin, M., Carlstrom, J. E., Chang, C. L., Cho, H. M., Clocchiatti, A., Crawford, T. M., Crites, A. T., Desai, S., Dobbs, M. A., Foley, R. J.,

Forman, W. R., George, E. M., Gladders, M. D., Gonzalez, A. H., Halverson, N. W., Harrington, N., High, F. W., Holder, G. P., Holzapfel, W. L., Hoover, S., Hrubes, J. D., Jones, C., Joy, M., Keisler, R., Knox, L., Lee, A. T., Leitch, E. M., Liu, J., Lueker, M., Luong-Van, D., Mantz, A., Marrone, D. P., McDonald, M., McMahon, J. J., Mehl, J., Meyer, S. S., Mocanu, L., Mohr, J. J., Montroy, T. E., Murray, S. S., Natoli, T., Padin, S., Plagge, T., Pryke, C., Rest, A., Ruel, J., Ruhl, J. E., Saliwanchik, B. R., Saro, A., Sayre, J. T., Schaffer, K. K., Shaw, L., Shirokoff, E., Song, J., Spieler, H. G., Stalder, B., Staniszewski, Z., Stark, A. A., Story, K., Stubbs, C. W., Suhada, R., van Engelen, A., Vanderlinde, K., Vieira, J. D., Vikhlinin, A., Williamson, R., Zahn, O., and Zenteno, A., "Cosmological Constraints from Sunyaev-Zel'dovich-selected Clusters with X-Ray Observations in the First 178 deg$^2$ of the South Pole Telescope Survey," *ApJ* **763**, 147 (Feb. 2013).

[13] Reichardt, C. L., Stalder, B., Bleem, L. E., Montroy, T. E., Aird, K. A., Andersson, K., Armstrong, R., Ashby, M. L. N., Bautz, M., Bayliss, M., Bazin, G., Benson, B. A., Brodwin, M., Carlstrom, J. E., Chang, C. L., Cho, H. M., Clocchiatti, A., Crawford, T. M., Crites, A. T., de Haan, T., Desai, S., Dobbs, M. A., Dudley, J. P., Foley, R. J., Forman, W. R., George, E. M., Gladders, M. D., Gonzalez, A. H., Halverson, N. W., Harrington, N. L., High, F. W., Holder, G. P., Holzapfel, W. L., Hoover, S., Hrubes, J. D., Jones, C., Joy, M., Keisler, R., Knox, L., Lee, A. T., Leitch, E. M., Liu, J., Lueker, M., Luong-Van, D., Mantz, A., Marrone, D. P., McDonald, M., McMahon, J. J., Mehl, J., Meyer, S. S., Mocanu, L., Mohr, J. J., Murray, S. S., Natoli, T., Padin, S., Plagge, T., Pryke, C., Rest, A., Ruel, J., Ruhl, J. E., Saliwanchik, B. R., Saro, A., Sayre, J. T., Schaffer, K. K., Shaw, L., Shirokoff, E., Song, J., Spieler, H. G., Staniszewski, Z., Stark, A. A., Story, K., Stubbs, C. W., Šuhada, R., van Engelen, A., Vanderlinde, K., Vieira, J. D., Vikhlinin, A., Williamson, R., Zahn, O., and Zenteno, A., "Galaxy Clusters Discovered via the Sunyaev-Zel'dovich Effect in the First 720 Square Degrees of the South Pole Telescope Survey," *ApJ* **763**, 127 (Feb. 2013).

[14] Vieira, J. D., Crawford, T. M., Switzer, E. R., Ade, P. A. R., Aird, K. A., Ashby, M. L. N., Benson, B. A., Bleem, L. E., Brodwin, M., Carlstrom, J. E., Chang, C. L., Cho, H., Crites, A. T., de Haan, T., Dobbs, M. A., Everett, W., George, E. M., Gladders, M., Hall, N. R., Halverson, N. W., High, F. W., Holder, G. P., Holzapfel, W. L., Hrubes, J. D., Joy, M., Keisler, R., Knox, L., Lee, A. T., Leitch, E. M., Lueker, M., Marrone, D. P., McIntyre, V., McMahon, J. J., Mehl, J., Meyer, S. S., Mohr, J. J., Montroy, T. E., Padin, S., Plagge, T., Pryke, C., Reichardt, C. L., Ruhl, J. E., Schaffer, K. K., Shaw, L., Shirokoff, E., Spieler, H. G., Stalder, B., Staniszewski, Z., Stark, A. A., Vanderlinde, K., Walsh, W., Williamson, R., Yang, Y., Zahn, O., and Zenteno, A., "Extragalactic Millimeter-wave Sources in South Pole Telescope Survey Data: Source Counts, Catalog, and Statistics for an 87 Square-degree Field," *ApJ* **719**, 763–783 (Aug. 2010).

[15] Vieira, J. D., Marrone, D. P., Chapman, S. C., De Breuck, C., Hezaveh, Y. D., Weiβ, A., Aguirre, J. E., Aird, K. A., Aravena, M., Ashby, M. L. N., Bayliss, M., Benson, B. A., Biggs, A. D., Bleem, L. E., Bock, J. J., Bothwell, M., Bradford, C. M., Brodwin, M., Carlstrom, J. E., Chang, C. L., Crawford, T. M., Crites, A. T., de Haan, T., Dobbs, M. A., Fomalont, E. B., Fassnacht, C. D., George, E. M., Gladders, M. D., Gonzalez, A. H., Greve, T. R., Gullberg, B., Halverson, N. W., High, F. W., Holder, G. P., Holzapfel, W. L., Hoover, S., Hrubes, J. D., Hunter, T. R., Keisler, R., Lee, A. T., Leitch, E. M., Lueker, M., Luong-van, D., Malkan, M., McIntyre, V., McMahon, J. J., Mehl, J., Menten, K. M., Meyer, S. S., Mocanu, L. M., Murphy, E. J., Natoli, T., Padin, S., Plagge, T., Reichardt, C. L., Rest, A., Ruel, J., Ruhl, J. E., Sharon, K., Schaffer, K. K., Shaw, L., Shirokoff, E., Spilker, J. S., Stalder, B., Staniszewski, Z., Stark, A. A., Story, K., Vanderlinde, K., Welikala, N., and Williamson, R., "Dusty starburst galaxies in the early Universe as revealed by gravitational lensing," *Nature* **495**, 344–347 (Mar. 2013).

[16] Mocanu, L. M., Crawford, T. M., Vieira, J. D., Aird, K. A., Aravena, M., Austermann, J. E., Benson, B. A., Béthermin, M., Bleem, L. E., Bothwell, M., Carlstrom, J. E., Chang, C. L., Chapman, S., Cho, H.-M., Crites, A. T., de Haan, T., Dobbs, M. A., Everett, W. B., George, E. M., Halverson, N. W., Harrington, N., Hezaveh, Y., Holder, G. P., Holzapfel, W. L., Hoover, S., Hrubes, J. D., Keisler, R., Knox, L., Lee, A. T., Leitch, E. M., Lueker, M., Luong-Van, D., Marrone, D. P., McMahon, J. J., Mehl, J., Meyer, S. S., Mohr, J. J., Montroy, T. E., Natoli, T., Padin, S., Plagge, T., Pryke, C., Rest, A., Reichardt, C. L., Ruhl, J. E., Sayre, J. T., Schaffer, K. K., Shirokoff, E., Spieler, H. G., Spilker, J. S., Stalder, B., Staniszewski, Z., Stark, A. A., Story, K. T., Switzer, E. R., Vanderlinde, K., and Williamson, R., "Extragalactic Millimeter-wave Point-source Catalog, Number Counts and Statistics from 771 deg$^2$ of the SPT-SZ Survey," *ApJ* **779**, 61 (Dec. 2013).

[17] Lueker, M., Reichardt, C. L., Schaffer, K. K., Zahn, O., Ade, P. A. R., Aird, K. A., Benson, B. A., Bleem, L. E., Carlstrom, J. E., Chang, C. L., Cho, H., Crawford, T. M., Crites, A. T., de Haan, T., Dobbs, M. A., George, E. M., Hall, N. R., Halverson, N. W., Holder, G. P., Holzapfel, W. L., Hrubes, J. D., Joy, M., Keisler, R., Knox, L., Lee, A. T., Leitch, E. M., McMahon, J. J., Mehl, J., Meyer, S. S., Mohr, J. J., Montroy, T. E., Padin, S., Plagge, T., Pryke, C., Ruhl, J. E., Shaw, L., Shirokoff, E., Spieler, H. G., Stalder, B., Staniszewski, Z., Stark, A. A., Vanderlinde, K., Vieira, J. D., and Williamson, R., "Measurements of Secondary Cosmic Microwave Background Anisotropies with the South Pole Telescope," *ApJ* **719**, 1045–1066 (Aug. 2010).

[18] Shirokoff, E., Reichardt, C. L., Shaw, L., Millea, M., Ade, P. A. R., Aird, K. A., Benson, B. A., Bleem, L. E., Carlstrom, J. E., Chang, C. L., Cho, H. M., Crawford, T. M., Crites, A. T., de Haan, T., Dobbs, M. A., Dudley, J., George, E. M., Halverson, N. W., Holder, G. P., Holzapfel, W. L., Hrubes, J. D., Joy, M., Keisler, R., Knox, L., Lee, A. T., Leitch, E. M., Lueker, M., Luong-Van, D., McMahon, J. J., Mehl, J., Meyer, S. S., Mohr, J. J., Montroy, T. E., Padin, S., Plagge, T., Pryke, C., Ruhl, J. E., Schaffer, K. K., Spieler, H. G., Staniszewski, Z., Stark, A. A., Story, K., Vanderlinde, K., Vieira, J. D., Williamson, R., and Zahn, O., "Improved Constraints on Cosmic Microwave Background Secondary Anisotropies from the Complete 2008 South Pole Telescope Data," *ApJ* **736**, 61–+ (July 2011).

[19] Keisler, R., Reichardt, C. L., Aird, K. A., Benson, B. A., Bleem, L. E., Carlstrom, J. E., Chang, C. L., Cho, H. M., Crawford, T. M., Crites, A. T., de Haan, T., Dobbs, M. A., Dudley, J., George, E. M., Halverson, N. W., Holder, G. P., Holzapfel, W. L., Hoover, S., Hou, Z., Hrubes, J. D., Joy, M., Knox, L., Lee, A. T., Leitch, E. M., Lueker, M., Luong-Van, D., McMahon, J. J., Mehl, J., Meyer, S. S., Millea, M., Mohr, J. J., Montroy, T. E., Natoli, T., Padin, S., Plagge, T., Pryke, C., Ruhl, J. E., Schaffer, K. K., Shaw, L., Shirokoff, E., Spieler, H. G., Staniszewski, Z., Stark, A. A., Story, K., van Engelen, A., Vanderlinde, K., Vieira, J. D., Williamson, R., and Zahn, O., "A Measurement of the Damping Tail of the Cosmic Microwave Background Power Spectrum with the South Pole Telescope," *ApJ* **743**, 28 (Dec. 2011).

[20] van Engelen, A., Keisler, R., Zahn, O., Aird, K. A., Benson, B. A., Bleem, L. E., Carlstrom, J. E., Chang, C. L., Cho, H. M., Crawford, T. M., Crites, A. T., de Haan, T., Dobbs, M. A., Dudley, J., George, E. M., Halverson, N. W., Holder, G. P., Holzapfel, W. L., Hoover, S., Hou, Z., Hrubes, J. D., Joy, M., Knox, L., Lee, A. T., Leitch, E. M., Lueker, M., Luong-Van, D., McMahon, J. J., Mehl, J., Meyer, S. S., Millea, M., Mohr, J. J., Montroy, T. E., Natoli, T., Padin, S., Plagge, T., Pryke, C., Reichardt, C. L., Ruhl, J. E., Sayre, J. T., Schaffer, K. K., Shaw, L., Shirokoff, E., Spieler, H. G., Staniszewski, Z., Stark, A. A., Story, K., Vanderlinde, K., Vieira, J. D., and Williamson, R., "A Measurement of Gravitational Lensing of the Microwave Background Using South Pole Telescope Data," *ApJ* **756**, 142 (Sept. 2012).

[21] Crawford, T. M., Schaffer, K. K., Bhattacharya, S., Aird, K. A., Benson, B. A., Bleem, L. E., Carlstrom, J. E., Chang, C. L., Cho, H.-M., Crites, A. T., de Haan, T., Dobbs, M. A., Dudley, J., George, E. M., Halverson, N. W., Holder, G. P., Holzapfel, W. L., Hoover, S., Hou, Z., Hrubes, J. D., Keisler, R., Knox, L., Lee, A. T., Leitch, E. M., Lueker, M., Luong-Van, D., McMahon, J. J., Mehl, J., Meyer, S. S., Millea, M., Mocanu, L. M., Mohr, J. J., Montroy, T. E., Padin, S., Plagge, T., Pryke, C., Reichardt, C. L., Ruhl, J. E., Sayre, J. T., Shaw, L., Shirokoff, E., Spieler, H. G., Staniszewski, Z., Stark, A. A., Story, K. T., van Engelen, A., Vanderlinde, K., Vieira, J. D., Williamson, R., and Zahn, O., "A measurement of the secondary-cmb and millimeter-wave-foreground bispectrum using 800deg2 of south pole telescope data," *The Astrophysical Journal* **784**(2), 143 (2014).

[22] Hanson, D., Hoover, S., Crites, A., Ade, P. A. R., Aird, K. A., Austermann, J. E., Beall, J. A., Bender, A. N., Benson, B. A., Bleem, L. E., Bock, J. J., Carlstrom, J. E., Chang, C. L., Chiang, H. C., Cho, H.-M., Conley, A., Crawford, T. M., de Haan, T., Dobbs, M. A., Everett, W., Gallicchio, J., Gao, J., George, E. M., Halverson, N. W., Harrington, N., Henning, J. W., Hilton, G. C., Holder, G. P., Holzapfel, W. L., Hrubes, J. D., Huang, N., Hubmayr, J., Irwin, K. D., Keisler, R., Knox, L., Lee, A. T., Leitch, E., Li, D., Liang, C., Luong-Van, D., Marsden, G., McMahon, J. J., Mehl, J., Meyer, S. S., Mocanu, L., Montroy, T. E., Natoli, T., Nibarger, J. P., Novosad, V., Padin, S., Pryke, C., Reichardt, C. L., Ruhl, J. E., Saliwanchik, B. R., Sayre, J. T., Schaffer, K. K., Schulz, B., Smecher, G., Stark, A. A., Story, K. T., Tucker, C., Vanderlinde, K., Vieira, J. D., Viero, M. P., Wang, G., Yefremenko, V., Zahn, O., and Zemcov, M., "Detection of B-Mode Polarization in the Cosmic Microwave Background with Data from the South Pole Telescope," *Physical Review Letters* **111**, 141301 (Oct. 2013).

[23] Abazajian, K. N., Arnold, K., Austermann, J., Benson, B. A., Bischoff, C., Bock, J., Bond, J. R., Borrill, J., Buder, I., Burke, D. L., Calabrese, E., Carlstrom, J. E., Carvalho, C. S., Chang, C. L., Chiang, H. C., Church, S., Cooray, A., Crawford, T. M., Crill, B. P., Dawson, K. S., Das, S., Devlin, M. J., Dobbs, M., Dodelson, S., Doré, O., Dunkley, J., Feng, J. L., Fraisse, A., Gallicchio, J., Giddings, S. B., Green, D., Halverson, N. W., Hanany, S., Hanson, D., Hildebrandt, S. R., Hincks, A., Hlozek, R., Holder, G., Holzapfel, W. L., Honscheid, K., Horowitz, G., Hu, W., Hubmayr, J., Irwin, K., Jackson, M., Jones, W. C., Kallosh, R., Kamionkowski, M., Keating, B., Keisler, R., Kinney, W., Knox, L., Komatsu, E., Kovac, J., Kuo, C.-L., Kusaka, A., Lawrence, C., Lee, A. T., Leitch, E., Linde, A., Linder, E., Lubin, P., Maldacena, J., Martinec, E., McMahon, J., Miller, A., Mukhanov, V., Newburgh, L., Niemack, M. D., Nguyen, H., Nguyen, H. T., Page, L., Pryke, C., Reichardt, C. L., Ruhl, J. E., Sehgal, N., Seljak, U., Senatore, L., Sievers, J., Silverstein, E., Slosar, A., Smith, K. M., Spergel, D., Staggs, S. T., Stark, A., Stompor, R., Vieregg, A. G., Wang, G., Watson, S., Wollack, E. J., Wu, W. L. K., Yoon, K. W., Zahn, O., and Zaldarriaga, M., "Inflation Physics from the Cosmic Microwave Background and Large Scale Structure," *ArXiv e-prints* (Sept. 2013).

[24] Abazajian, K. N., Arnold, K., Austermann, J., Benson, B. A., Bischoff, C., Bock, J., Bond, J. R., Borrill, J., Calabrese, E., Carlstrom, J. E., Carvalho, C. S., Chang, C. L., Chiang, H. C., Church, S., Cooray, A., Crawford, T. M., Dawson, K. S., Das, S., Devlin, M. J., Dobbs, M., Dodelson, S., Dore, O., Dunkley, J., Errard, J., Fraisse, A., Gallicchio, J., Halverson, N. W., Hanany, S., Hildebrandt, S. R., Hincks, A., Hlozek, R., Holder, G., Holzapfel, W. L., Honscheid, K., Hu, W., Hubmayr, J., Irwin, K., Jones, W. C., Kamionkowski, M., Keating, B., Keisler, R., Knox, L., Komatsu, E., Kovac, J., Kuo, C.-L., Lawrence, C., Lee, A. T., Leitch, E., Linder, E., Lubin, P., McMahon, J., Miller, A., Newburgh, L., Niemack, M. D., Nguyen, H., Nguyen, H. T., Page, L., Pryke, C., Reichardt, C. L., Ruhl, J. E., Sehgal, N., Seljak, U., Sievers, J., Silverstein, E., Slosar, A., Smith, K. M., Spergel, D., Staggs, S. T., Stark, A., Stompor, R., Vieregg, A. G., Wang, G., Watson, S., Wollack, E. J., Wu, W. L. K., Yoon, K. W., and Zahn, O., "Neutrino Physics from the Cosmic Microwave Background and Large Scale Structure," *ArXiv e-prints* (Sept. 2013).

[25] Nguyen, H. T., Kovac, J., Ade, P., Aikin, R., Benton, S., Bock, J., Brevik, J., Carlstrom, J., Dowell, D., Duband, L., Golwala, S., Halpern, M., Hasslefield, M., Irwin, K., Jones, W., Kaufman, J., Keating, B., Kuo, C.-L., Lange, A., Matsumura, T., Netterfield, B., Pryke, C., Ruhl, J., Sheehy, C., and Sudiwala, R., "BICEP2/SPUD: searching for inflation with degree scale polarimetry from the South Pole," in [*Millimeter and Submillimeter Detectors and Instrumentation for Astronomy IV. Edited by Duncan, William D.; Holland, Wayne S.; Withington, Stafford; Zmuidzinas, Jonas. Proceedings of the SPIE, Volume 7020, pp. 70201F-70201F-9 (2008).*], **7020** (Aug. 2008).

[26] BICEP2 Collaboration, Ade, P. A. R., Aikin, R. W., Amiri, M., Barkats, D., Benton, S. J., Bischoff, C. A., Bock, J. J., Brevik, J. A., Buder, I., Bullock, E., Davis, G., Dowell, C. D., Duband, L., Filippini, J. P., Fliescher, S., Golwala, S. R., Halpern, M., Hasselfield, M., Hildebrandt, S. R., Hilton, G. C., Hristov, V. V., Irwin, K. D., Karkare, K. S., Kaufman, J. P., Keating, B. G., Kernasovskiy, S. A., Kovac, J. M., Kuo, C. L., Leitch, E. M., Llombart, N., Lueker, M., Netterfield, C. B., Nguyen, H. T., O'Brient, R., Ogburn, IV, R. W., Orlando, A., Pryke, C., Reintsema, C. D., Richter, S., Schwarz, R., Sheehy, C. D., Staniszewski, Z. K., Story, K. T., Sudiwala, R. V., Teply, G. P., Tolan, J. E., Turner, A. D., Vieregg, A. G., Wilson, P., Wong, C. L., and Yoon, K. W., "BICEP2 II: Experiment and Three-Year Data Set," *ArXiv e-prints* (Mar. 2014).

[27] Essinger-Hileman, T., Appel, J. W., Beall, J. A., Cho, H. M., Fowler, J., Halpern, M., Hasselfield, M., Irwin, K. D., Marriage, T. A., Niemack, M. D., Page, L., Parker, L. P., Pufu, S., Staggs, S. T., Stryzak, O., Visnjic, C., Yoon, K. W., and Zhao, Y., "The Atacama B-Mode Search: CMB Polarimetry with Transition-Edge-Sensor Bolometers," *AIP Conference Proceedings* **1185**(1), 494–497 (2009).

[28] Filippini, J. P., Ade, P. A. R., Amiri, M., Benton, S. J., Bihary, R., Bock, J. J., Bond, J. R., Bonetti, J. A., Bryan, S. A., Burger, B., Chiang, H. C., Contaldi, C. R., Crill, B. P., Doré, O., Farhang, M., Fissel, L. M., Gandilo, N. N., Golwala, S. R., Gudmundsson, J. E., Halpern, M., Hasselfield, M., Hilton, G., Holmes, W., Hristov, V. V., Irwin, K. D., Jones, W. C., Kuo, C. L., MacTavish, C. J., Mason, P. V., Montroy, T. E., Morford, T. A., Netterfield, C. B., O'Dea, D. T., Rahlin, A. S., Reintsema, C. D., Ruhl, J. E., Runyan, M. C., Schenker, M. A., Shariff, J. A., Soler, J. D., Trangsrud, A., Tucker, C., Tucker, R. S., and Turner, A. D., "SPIDER: a balloon-borne CMB polarimeter fkeor large angular scales," in [*Millimeter, Submillimeter, and*

*Far-Infrared Detectors and Instrumentation for Astronomy V. Edited by Holland, Wayne S.; Zmuidzinas, Jonas. Proceedings of the SPIE, Volume 7741, pp. 77411N-77411N-12 (2010).*], **7741** (July 2010).

[29] Reichborn-Kjennerud, B., Aboobaker, A. M., Ade, P., Aubin, F., Baccigalupi, C., Bao, C., Borrill, J., Cantalupo, C., Chapman, D., Didier, J., Dobbs, M., Grain, J., Grainger, W., Hanany, S., Hillbrand, S., Hubmayr, J., Jaffe, A., Johnson, B., Jones, T., Kisner, T., Klein, J., Korotkov, A., Leach, S., Lee, A., Levinson, L., Limon, M., MacDermid, K., Matsumura, T., Meng, X., Miller, A., Milligan, M., Pascale, E., Polsgrove, D., Ponthieu, N., Raach, K., Sagiv, I., Smecher, G., Stivoli, F., Stompor, R., Tran, H., Tristram, M., Tucker, G. S., Vinokurov, Y., Yadav, A., Zaldarriaga, M., and Zilic, K., "EBEX: a balloon-borne CMB polarization experiment," in [*Society of Photo-Optical Instrumentation Engineers (SPIE) Conference Series*], *Society of Photo-Optical Instrumentation Engineers (SPIE) Conference Series* **7741** (July 2010).

[30] Niemack, M. D., Ade, P. A. R., Aguirre, J., Barrientos, F., Beall, J. A., Bond, J. R., Britton, J., Cho, H. M., Das, S., Devlin, M. J., Dicker, S., Dunkley, J., Dünner, R., Fowler, J. W., Hajian, A., Halpern, M., Hasselfield, M., Hilton, G. C., Hilton, M., Hubmayr, J., Hughes, J. P., Infante, L., Irwin, K. D., Jarosik, N., Klein, J., Kosowsky, A., Marriage, T. A., McMahon, J., Menanteau, F., Moodley, K., Nibarger, J. P., Nolta, M. R., Page, L. A., Partridge, B., Reese, E. D., Sievers, J., Spergel, D. N., Staggs, S. T., Thornton, R., Tucker, C., Wollack, E., and Yoon, K. W., "ACTPol: a polarization-sensitive receiver for the Atacama Cosmology Telescope," in [*Society of Photo-Optical Instrumentation Engineers (SPIE) Conference Series*], *Arxiv e-prints* **7741** (July 2010).

[31] Arnold, K., Ade, P. A. R., Anthony, A. E., Aubin, F., Boettger, D., Borrill, J., Cantalupo, C., Dobbs, M. A., Errard, J., Flanigan, D., Ghribi, A., Halverson, N., Hazumi, M., Holzapfel, W. L., Howard, J., Hyland, P., Jaffe, A., Keating, B., Kisner, T., Kermish, Z., Lee, A. T., Linder, E., Lungu, M., Matsumura, T., Miller, N., Meng, X., Myers, M., Nishino, H., O'Brient, R., O'Dea, D., Reichardt, C., Schanning, I., Shimizu, A., Shimmin, C., Shimon, M., Spieler, H., Steinbach, B., Stompor, R., Suzuki, A., Tomaru, T., Tran, H. T., Tucker, C., Quealy, E., Richards, P. L., and Zahn, O., "The POLARBEAR CMB polarization experiment," in [*Society of Photo-Optical Instrumentation Engineers (SPIE) Conference Series*], *Society of Photo-Optical Instrumentation Engineers (SPIE) Conference Series* **7741** (July 2010).

[32] BICEP2 Collaboration, Ade, P. A. R., Aikin, R. W., Barkats, D., Benton, S. J., Bischoff, C. A., Bock, J. J., Brevik, J. A., Buder, I., Bullock, E., Dowell, C. D., Duband, L., Filippini, J. P., Fliescher, S., Golwala, S. R., Halpern, M., Hasselfield, M., Hildebrandt, S. R., Hilton, G. C., Hristov, V. V., Irwin, K. D., Karkare, K. S., Kaufman, J. P., Keating, B. G., Kernasovskiy, S. A., Kovac, J. M., Kuo, C. L., Leitch, E. M., Lueker, M., Mason, P., Netterfield, C. B., Nguyen, H. T., O'Brient, R., Ogburn, IV, R. W., Orlando, A., Pryke, C., Reintsema, C. D., Richter, S., Schwarz, R., Sheehy, C. D., Staniszewski, Z. K., Sudiwala, R. V., Teply, G. P., Tolan, J. E., Turner, A. D., Vieregg, A. G., Wong, C. L., and Yoon, K. W., "BICEP2 I: Detection Of B-mode Polarization at Degree Angular Scales," *ArXiv e-prints* (Mar. 2014).

[33] Seljak, U. and Hirata, C. M., "Gravitational lensing as a contaminant of the gravity wave signal in the CMB," *Phys. Rev. D* **69**, 043005–+ (Feb. 2004).

[34] Smith, T. L., Das, S., and Zahn, O., "Constraints on neutrino and dark radiation interactions using cosmological observations," *Phys. Rev. D* **85**, 023001 (Jan. 2012).

[35] Hu, W., Hedman, M. M., and Zaldarriaga, M., "Benchmark parameters for CMB polarization experiments," *Phys. Rev. D* **67**, 043004–+ (Feb. 2003). astro-ph/0210096.

[36] Wolf, J., "The katrin neutrino mass experiment," *Nuclear Instruments and Methods in Physics Research Section A: Accelerators, Spectrometers, Detectors and Associated Equipment* **623**(1), 442 – 444 (2010).

[37] Battistelli, E. S., Amico, G., Baù, A., Bergé, L., Bréelle, É., Charlassier, R., Collin, S., Cruciani, A., de Bernardis, P., Dufour, C., Dumoulin, L., Gervasi, M., Giard, M., Giordano, C., Giraud-Héraud, Y., Guglielmi, L., Hamilton, J.-C., Landé, J., Maffei, B., Maiello, M., Marnieros, S., Masi, S., Passerini, A., Piacentini, F., Piat, M., Piccirillo, L., Pisano, G., Polenta, G., Rosset, C., Salatino, M., Schillaci, A., Sordini, R., Spinelli, S., Tartari, A., and Zannoni, M., "Intensity and polarization of the atmospheric emission at millimetric wavelengths at Dome Concordia," *MNRAS* , 3009 (May 2012).

[38] Crawford, T., "Power spectrum sensitivity of raster-scanned CMB experiments in the presence of 1/f noise," *Phys. Rev. D* **76**, 063008–+ (Sept. 2007).

[39] Chiang, H. C., Ade, P. A. R., Barkats, D., Battle, J. O., Bierman, E. M., Bock, J. J., Dowell, C. D., Duband, L., Hivon, E. F., Holzapfel, W. L., Hristov, V. V., Jones, W. C., Keating, B. G., Kovac, J. M., Kuo, C. L., Lange, A. E., Leitch, E. M., Mason, P. V., Matsumura, T., Nguyen, H. T., Ponthieu, N., Pryke, C., Richter, S., Rocha, G., Sheehy, C., Takahashi, Y. D., Tolan, J. E., and Yoon, K. W., "Measurement of Cosmic Microwave Background Polarization Power Spectra from Two Years of BICEP Data," *ApJ* **711**, 1123–1140 (Mar. 2010).

[40] The Planck Collaboration, "The Scientific Programme of Planck," *ArXiv:astro-ph/0604069* (Apr. 2006).

[41] Seiffert, M., Borys, C., Scott, D., and Halpern, M., "An upper limit to polarized submillimetre emission in Arp 220," *MNRAS* **374**, 409–414 (Jan. 2007).

[42] Pillepich, A., Porciani, C., and Reiprich, T. H., "The X-ray cluster survey with eRosita: forecasts for cosmology, cluster physics and primordial non-Gaussianity," *MNRAS* **422**, 44–69 (May 2012).

[43] Keisler, R. and Schmidt, F., "Prospects for Measuring the Relative Velocities of Galaxy Clusters in Photometric Surveys Using the Kinetic Sunyaev-Zel'dovich Effect," *ApJL* **765**, L32 (Mar. 2013).

[44] Planck Collaboration, Ade, P. A. R., Aghanim, N., Arnaud, M., Ashdown, M., Aumont, J., Baccigalupi, C., Balbi, A., Banday, A. J., Barreiro, R. B., and et al., "Planck early results. VIII. The all-sky early Sunyaev-Zeldovich cluster sample," *A&A* **536**, A8 (Dec. 2011).

[45] Wu, H.-Y., Rozo, E., and Wechsler, R. H., "Annealing a Follow-up Program: Improvement of the Dark Energy Figure of Merit for Optical Galaxy Cluster Surveys," *ApJ* **713**, 1207–1218 (Apr. 2010).

[46] Rozo, E., Wu, H.-Y., and Schmidt, F., "Stacked Weak Lensing Mass Calibration: Estimators, Systematics, and Impact on Cosmological Parameter Constraints," *ApJ* **735**, 118 (July 2011).

[47] Dodelson, S., "CMB-cluster lensing," *Phys. Rev. D* **70**, 023009 (July 2004).

[48] Hu, W., DeDeo, S., and Vale, C., "Cluster mass estimators from CMB temperature and polarization lensing," *New Journal of Physics* **9**, 441–+ (Dec. 2007).

[49] Hand, N., Addison, G. E., Aubourg, E., Battaglia, N., Battistelli, E. S., Bizyaev, D., Bond, J. R., Brewington, H., Brinkmann, J., Brown, B. R., Das, S., Dawson, K. S., Devlin, M. J., Dunkley, J., Dunner, R., Eisenstein, D. J., Fowler, J. W., Gralla, M. B., Hajian, A., Halpern, M., Hilton, M., Hincks, A. D., Hlozek, R., Hughes, J. P., Infante, L., Irwin, K. D., Kosowsky, A., Lin, Y.-T., Malanushenko, E., Malanushenko, V., Marriage, T. A., Marsden, D., Menanteau, F., Moodley, K., Niemack, M. D., Nolta, M. R., Oravetz, D., Page, L. A., Palanque-Delabrouille, N., Pan, K., Reese, E. D., Schlegel, D. J., Schneider, D. P., Sehgal, N., Shelden, A., Sievers, J., Sifon, C., Simmons, A., Snedden, S., Spergel, D. N., Staggs, S. T., Swetz, D. S., Switzer, E. R., Trac, H., Weaver, B. A., Wollack, E. J., Yeche, C., and Zunckel, C., "Detection of Galaxy Cluster Motions with the Kinematic Sunyaev-Zel'dovich Effect," *ArXiv:1203.4219* (Mar. 2012).

[50] Karpov, A., Miller, D., Rice, F. R., Stern, J. A., Bumble, B., LeDuc, H. G., and Zmuidzinas, J., "Low-noise SIS mixer for far-infrared radio astronomy," in [*Society of Photo-Optical Instrumentation Engineers (SPIE) Conference Series*], Bradford, C. M., Ade, P. A. R., Aguirre, J. E., Bock, J. J., Dragovan, M., Duband, L., Earle, L., Glenn, J., Matsuhara, H., Naylor, B. J., Nguyen, H. T., Yun, M., and Zmuidzinas, J., eds., *Society of Photo-Optical Instrumentation Engineers (SPIE) Conference Series* **5498**, 616–621 (Oct. 2004).

[51] POLARBEAR Collaboration, Ade, P. A. R., Akiba, Y., Anthony, A. E., Arnold, K., Atlas, M., Barron, D., Boettger, D., Borrill, J., Chapman, S., Chinone, Y., Dobbs, M., Elleflot, T., Errard, J., Fabbian, G., Feng, C., Flanigan, D., Gilbert, A., Grainger, W., Halverson, N. W., Hasegawa, M., Hattori, K., Hazumi, M., Holzapfel, W. L., Hori, Y., Howard, J., Hyland, P., Inoue, Y., Jaehnig, G. C., Jaffe, A., Keating, B., Kermish, Z., Keskitalo, R., Kisner, T., Le Jeune, M., Lee, A. T., Linder, E., Leitch, E. M., Lungu, M., Matsuda, F., Matsumura, T., Meng, X., Miller, N. J., Morii, H., Moyerman, S., Myers, M. J., Navaroli, M., Nishino, H., Paar, H., Peloton, J., Quealy, E., Rebeiz, G., Reichardt, C. L., Richards, P. L., Ross, C., Schanning, I., Schenck, D. E., Sherwin, B., Shimizu, A., Shimmin, C., Shimon, M., Siritanasak, P., Smecher, G., Spieler, H., Stebor, N., Steinbach, B., Stompor, R., Suzuki, A., Takakura, S., Tomaru, T., Wilson, B., Yadav, A., and Zahn, O., "Measurement of the Cosmic Microwave Background Polarization Lensing Power Spectrum with the POLARBEAR experiment," *ArXiv e-prints* (Dec. 2013).

[52] Ade, P. A. R., Akiba, Y., Anthony, A. E., Arnold, K., Atlas, M., Barron, D., Boettger, D., Borrill, J., Borys, C., Chapman, S., Chinone, Y., Dobbs, M., Elleflot, T., Errard, J., Fabbian, G., Feng, C., Flanigan, D., Gilbert, A., Grainger, W., Halverson, N. W., Hasegawa, M., Hattori, K., Hazumi, M., Holzapfel, W. L.,

Hori, Y., Howard, J., Hyland, P., Inoue, Y., Jaehnig, G. C., Jaffe, A., Keating, B., Kermish, Z., Keskitalo, R., Kisner, T., Le Jeune, M., Lee, A. T., Leitch, E. M., Linder, E., Lungu, M., Matsuda, F., Matsumura, T., Meng, X., Miller, N. J., Morii, H., Moyerman, S., Myers, M. J., Navaroli, M., Nishino, H., Paar, H., Peloton, J., Poletti, D., Quealy, E., Rebeiz, G., Reichardt, C. L., Richards, P. L., Ross, C., Rotermund, K., Schanning, I., Schenck, D. E., Sherwin, B. D., Shimizu, A., Shimmin, C., Shimon, M., Siritanasak, P., Smecher, G., Spieler, H., Stebor, N., Steinbach, B., Stompor, R., Suzuki, A., Takakura, S., Tikhomirov, A., Tomaru, T., Wilson, B., Yadav, A., Zahn, O., and Polarbear Collaboration, "Evidence for Gravitational Lensing of the Cosmic Microwave Background Polarization from Cross-Correlation with the Cosmic Infrared Background," *Physical Review Letters* **112**, 131302 (Apr. 2014).

[53] Suzuki, A., Arnold, K., Edwards, J., Engargiola, G., Ghribi, A., Holzapfel, W., Lee, A., Meng, X., Myers, M., OBrient, R., Quealy, E., Rebeiz, G., and Richards, P., "Multi-chroic dual-polarization bolometric focal plane for studies of the cosmic microwave background," *Journal of Low Temperature Physics* **167**, 852–858 (2012).

[54] Dobbs, M., Bissonnette, E., and Spieler, H., "Digital Frequency Domain Multiplexer for Millimeter-Wavelength Telescopes," *IEEE Transactions on Nuclear Science* **55**, 21–26 (2008).

[55] Dobbs, M. A., Lueker, M., Aird, K. A., Bender, A. N., Benson, B. A., Bleem, L. E., Carlstrom, J. E., Chang, C. L., Cho, H.-M., Clarke, J., Crawford, T. M., Crites, A. T., Flanigan, D. I., de Haan, T., George, E. M., Halverson, N. W., Holzapfel, W. L., Hrubes, J. D., Johnson, B. R., Joseph, J., Keisler, R., Kennedy, J., Kermish, Z., Lanting, T. M., Lee, A. T., Leitch, E. M., Luong-Van, D., McMahon, J. J., Mehl, J., Meyer, S. S., Montroy, T. E., Padin, S., Plagge, T., Pryke, C., Richards, P. L., Ruhl, J. E., Schaffer, K. K., Schwan, D., Shirokoff, E., Spieler, H. G., Staniszewski, Z., Stark, A. A., Vanderlinde, K., Vieira, J. D., Vu, C., Westbrook, B., and Williamson, R., "Frequency Multiplexed SQUID Readout of Large Bolometer Arrays for Cosmic Microwave Background Measurements," *"Rev. Sci. Instrum.* **83** (July 2012).

[56] Dobbs, M., Aubin, F., de Haan, T., Hanany, S., Harrington, N., Holzapfel, W., Hubmayr, J., Lee, A., Lueker, M., Macdermid, K., and Smecher, G., "Digital Frequency Multiplexer for TES Detectors Path to Flight," *Journal of Low Temperature Physics* **167**, 568–574 (June 2012).

[57] de Haan, T., Smecher, G., and Dobbs, M., "Improved performance of TES bolometers using digital feedback," in [*Society of Photo-Optical Instrumentation Engineers (SPIE) Conference Series*], *Society of Photo-Optical Instrumentation Engineers (SPIE) Conference Series* **8452** (Sept. 2012).